CrossMark

Improving seismic hazard approaches for critical infrastructures: a pilot study in the Po Plain

M. Vanini[1] · M. Corigliano[2] · E. Faccioli[3] · R. Figini[4] ·
L. Luzi[5] · F. Pacor[5] · R. Paolucci[1]

Abstract Paper describes the extensive work done in the SIGMA project, aimed at improving knowledge on data, methods and tools to better quantify uncertainties in seismic hazard assessment (SHA). The authors cooperated in the study of potential faults and geological structures, earthquake catalogues, selection of ground motion prediction equations, and methods for site effect evaluation suitable for SHA. All the contributions merged into a probabilistic seismic hazard study conducted for three representative sites of the Po Plain in Northern Italy. Po Plain is a low-to-moderate seismicity region, characterized by some critical features, such as blind faulting and deep alluvium sediments, and by scarcity of strong motion data; these sources of uncertainties in seismic hazard estimation are common to other low seismicity areas around the world. Within SIGMA, special care was devoted to: (a) the use of the single station sigma approach inside the probabilistic SHA, (b) the comparative use of generalized attenuation functions to evaluate the hazard contribution of composite fault systems, and (c) the study of the epistemic uncertainties at play when different modelling approaches to site effects are used.

Keywords Probabilistic seismic hazard analysis · Single station sigma · Uncertainties quantification · Po Plain · Site effects

E. Faccioli was formerly at Politecnico di Milano.

The original version of this article was revised: In the initial online publication the top-right graph of figure 21 was the same as the top-left figure. This has been corrected.

✉ M. Vanini
 mm.vanini@gmail.com

1 Politecnico di Milano, Piazza Leonardo da Vinci 32, 20133 Milan, Italy

2 ENEL, Via Carducci 1/3, 20123 Milan, Italy

3 Studio Geotecnico Italiano, Via Giuseppe Ripamonti, 89, Milan, Italy

4 ENEL, Via Adamello 5, 20099 Sesto San Giovanni, Milan, Italy

5 Istituto Nazionale di Geofisica e Vulcanologia (INGV), Sezione di Milano, Via Corti 12, 20133 Milan, Italy

 Springer

1 Introduction

Nuclear power plants (NPPs), large dams, petrochemical installations, liquid natural gas (LNG) terminals, major bridges, etc. represent a few examples of critical infrastructures whose design requires a detailed seismic hazard (SH) assessment in order to quantify the associated risk. Critical infrastructures are structures or systems characterized by a high potential to cause loss of human life, serious property damage or destruction of socio-economic activities with strong economic impact.

Among the critical infrastructures, a special role is played by the NPPs due to the impact that an accident may produce. Because of this, NPPs have also been the most thoroughly studied and those that have contributed to produce the most advanced studies in SH assessment. Recent examples are the PEGASOS project in Switzerland (Renault 2014) and the Thyspunt project in South Africa (Bommer et al. 2015).

PEGASOS, carried out between 2000 and 2004, was aimed at the quantification of epistemic uncertainty and aleatory variability in SH for Switzerland. After its completion, a refinement process (PEGASOS Refinement Project, PRP) was launched in 2008, finalized to further reducing the identified uncertainties, accounting for the new developments and the newly available data (especially in the field of ground motion modelling). PRP was subdivided into different tasks (Sub-Projects), concerning the characterization of the seismic source, the ground motion and the site response, and the calculation of hazard and resulting scenario earthquakes (Swissnuclear 2013).

The most significant PRP results in terms of uncertainty characterization can be synthesized as follows (Renault 2014): (a) refinements of the source geometry characterization would not lead to significant reductions in the epistemic uncertainty of the hazard, while refinements in earthquake catalog and of distributions of the maximum magnitude of the source zones are among the most important parameters controlling the hazard results. (b) The ground motion characterization introduces the most significant contribution to the epistemic uncertainty in the SH. PRP accounted for significant advances in the ground motion field, with new prediction models made available and new models for the uncertainty (sigma) of the GMPEs based on the single-station sigma approach (Rodriguez-Marek et al. 2011). (c) PRP results on site effects showed that shear-wave velocity profile and material properties (i.e. shear modulus and damping) are the most important model parameters controlling the hazard results.

The PEGASOS and Thyspunt projects well represent the attempts recently made at identifying and quantifying uncertainties in SH estimation for low-to-moderate seismicity areas, typically chosen in NPP siting, highlighting the difficulties created by the lack of representative data. The ensuing difficulties in defining the design and verification levels of the seismic action can give rise to different interpretations and divergent opinions among experts (Senfaute 2012).

The results presented herein, obtained in the framework of SIGMA, illustrate the contributions of the Italian team of researchers which focused on the Po Plain basin.

The Po Plain is a densely populated and highly industrialized region of Northern Italy, sitting on a large alluvium basin filled by very deep Quaternary sediments with flat surface topography and strongly variable total thickness, with earthquakes originating from blind faults in the rock basement, as well as at greater depths (up to several tens of km). The basin, with the adjacent portions of Northern Apennines to the South and of the Central Alps to the North, is exposed to moderate seismic activity, significantly less intense than the Central and Southern Apennines, but far from negligible. The seismicity of Northern Italy is generally characterized by the occurrence of small energy events (about 200/year)

and by infrequent moderate earthquakes. This is confirmed by the repeated earthquakes in the M_W 5-to-6 magnitude range over the last few years, most notably the damaging 2012 Emilia seismic sequence. This struck the Northern Italy provinces of Modena and Ferrara in May–June 2012 with significant social and economic impact, and was characterized by two mainshocks (May 20 and 29, 2012) of $M_W \sim 6$, six more shocks with $M_W > 5.0$ (ITalian ACcelerometric Archive, ITACA Working Group 2016), and about 2500 located smaller earthquakes (Italian seismological Instrumental and Parametric Database, ISIDe Working Group 2016).

During the sequence a vast amount of geological, seismological, geophysical and geotechnical information was collected through instrumental records, and field surveys and measurements, which now constitutes an important case study that can strongly contribute to refining and possibly reducing uncertainties in SH assessment.

Despite to the low-to-moderate seismicity of the Po Plain, the definition of the site-specific SH on it poses a significant challenge, especially when considering low occurrence probabilities. Part of the challenge stems from the lack of morphological surface evidence on earthquake sources (blind faulting). Moreover, the variability introduced by site effects on deep recent sediments may make a realistic estimation of the SH more difficult. This work is not intended to produce a review of any hazard map or of site-specific hazard evaluations, but rather to delve more deeply into key modelling issues likely to influence the SH analysis, and arising from the characterization of blind faults, the scarcity of earthquake data and the estimation of site effects induced by deep sedimentary deposits. The analyses presented should be seen as path markers towards a better appraisal of the uncertainties involved and, possibly, towards their reduction in future studies. After reviewing in the next section the seismotectonic setting of the Po Plain, empirical ground motion models are discussed, followed by the SH assessment proper. Three representative sites were chosen for the PSHA, not as potentially interesting locations for industrial facilities, but rather because they were well instrumented, so that data recorded during recent earthquakes could be used within the analyses.

2 Seismotectonics

In principle, both the characterization of potentially active geological structures and the update of the earthquake catalogue were WP1 tasks. In the framework of the Italian WP1 activities most of the effort was concentrated on the first task because a good quality catalogue of Italian earthquakes, i.e. CPTI04 (Gruppo di lavoro CPTI 2004), already existed at the start of Sigma catalogue. However, a specific study has been devoted within WP1 to the uncertainty related to the parametrization of historical intensity data, briefly discussed in Sect. 2.5. The use of the Earthquake catalogue will be more extensively treated in Sect. 4, where the WP4 activities concerning SH assessment are described.

2.1 Structural setting

The Po Plain is the largest alluvium plain in Italy. Its peculiarity is the elevation contrast with the Alps and the Apennines, the mountain chains surrounding it (Fig. 1). The Po Plain is the foreland area of two opposing verging fold-and-thrust belts: to the North, the S-verging central Southern Alps, and to the South the N–NE-verging Northern Apennines. The outcropping portions of these two chains define the structural and morphological
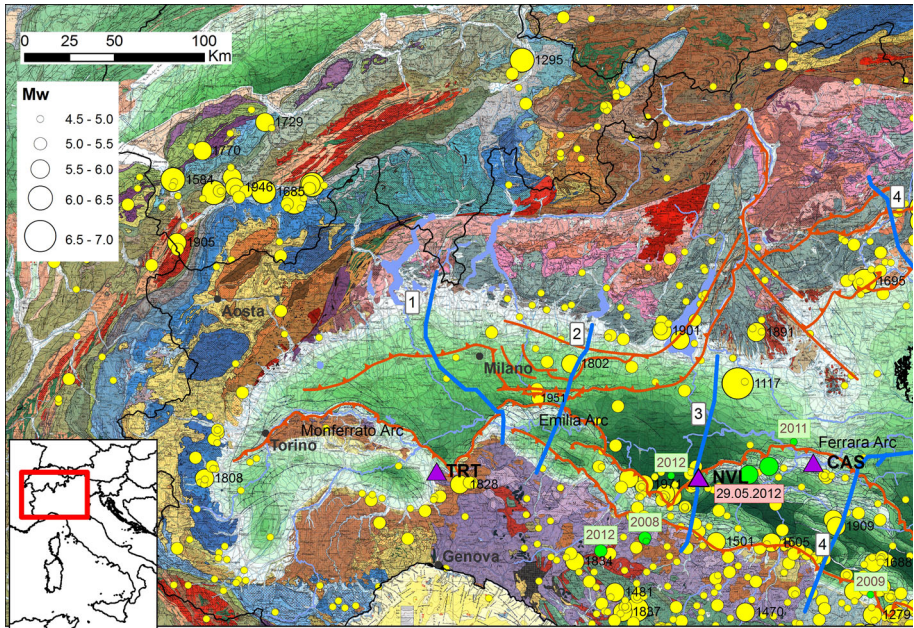
Fig. 1 In background, structural model of Northwestern Italy [from Bigi et al. (1992)] showing the main tectonic elements of the Southern Alps (to the North) and Northern Apennines (to the South) chains. The *green color palette* defines the depth of the base of the Plio-Quaternary succession in the plain, which highlights the deformation associated with the outermost thrust fronts of the two chains (*orange lines*). *Blue lines* are the traces of the seismic sections of Fantoni and Franciosi (2010); Sect. 3 is shown in Fig. 2. Historical seismicity is shown as well. Earthquake epicenters are taken from the Parametric Catalogue of Italian Earthquakes CPTI11 (Rovida et al. 2011), from 1005 up to 2006, shown by *yellow symbols*, and from the ISIDe database for the events up to 2012, *green symbols*. Location and date of some earlier 2008, 2011 and 2012 events in the M ∼5 range are highlighted. *Purple triangles* show the reference sites of this study: from West to East these are Tortona (TRT), Novellara (NVL) and Casaglia (CAS)

margins of the plain itself, but their outermost thrusts are not confined at the mountain fronts, and are today buried by the Plio-Quaternary sediments that fill in the Po Plain (Figs. 1, 2). The two belts developed during the closure of the Mesozoic Tethyan basin occurring in the framework of the relative convergence between the African and European plates from the Cretaceous onward, and were associated with two opposite subduction zones involving both European and African lithosphere (Carminati and Doglioni 2012).
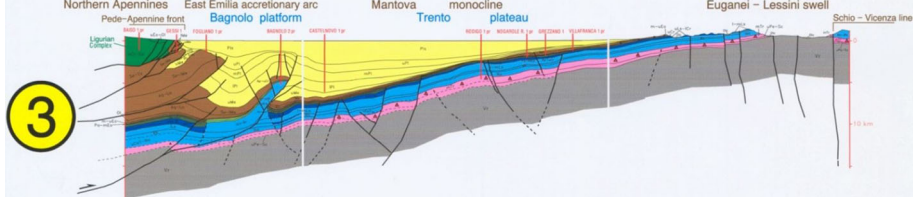

Fig. 2 N–S trending, depth-converted seismic section showing the deep geometry of the Northern Apennines and of the Southern Alps thrust belts [from Fantoni and Franciosi (2010), modified]. Trace of this section shown in Fig. 1

The outermost thrust fronts of the Northern Apennines belt, buried below the Plio-Quaternary marine and continental deposits in-filling the Po Plain basin, are organized in three complex system of folds: the Monferrato, the Emilian and the Ferrara arcs, from West to East (Fig. 1). The buried compressional structures were extensively explored by seismic reflection lines and deep well logs. These subsurface data show a system of N–NE-verging blind thrusts and folds that controlled the deposition of the syntectonic sedimentary wedges, overlain by a Plio-Quaternary sequence locally up to 7–8 km thick.

2.2 Seismicity

The seismicity of the Po Plain, which can be described through the records of both the historical CPTI11 catalogue (Rovida et al. 2011) and the instrumental ones (Pondrelli et al. 2011), is generally characterized by the occurrence of infrequent moderate earthquakes. The general pattern of the historical seismicity shows that most of the earthquakes which affected the Po Plain originated south of the Po River (Fig. 1), and provides evidence of the activity of the Northern Apenninic thrusts, along both the pede-appeninic margin and the buried fronts inside the Po Plain.

The distribution of low to moderate earthquakes south of the Po River fits well with the position and geometry of the three main frontal arcs of the Northern Apennines noted in Fig. 1 (Monferrato, Emilia and Ferrara arcs), with higher energy release in the easternmost arc. In this respect, a general observation is that the number of earthquakes consistently decreases moving from the eastern (Friuli plain) to the western (Piedmont) margin of the Po Plain. The data are in agreement with the general geodynamic setting of the Northern Apennines-Adria-Southern Alps convergent system and with GPS velocity data. The latter show that the Adria plate is moving towards the European continent with nearly N-directed velocity vectors and faster to the East. The pole of rotation lies in the Western Alps, where the convergence is absent. For this reason the activity of the thrust structures is more significant in the eastern Southern Alps and in the Ferrara arc with respect to the western Southern Alps belts and the Monferrato arc front.

Inspection of the instrumental earthquake catalogue offers important information concerning the earthquake depth distribution. Most of the events are located in the uppermost 15 km of the crust (see Fig. 3). Based on the structural setting of the region one can infer that the events are generated inside the orogenic wedges if they fall within the upper 15 km, whereas those falling between 15 and 30 km depth are mainly located inside the crustal portion of the Adria plate. Deeper earthquakes (>30 km) occur as well, and cannot be neglected in drawing a reliable seismotectonic framework of Northern Italy. They are probably related to the flexure of the Adria plate under the Apennine orogen. Available data allow to outline the geometry of the lithosphere sinking under the Tyrrhenian crust as a "slab" dipping approximately 20° towards SW, between the Po Plain and the peri-Tyrrhenian area, see Fig. 3.

2.3 Seismogenic sources in Po Plain

The significant Italian earthquake sources are described in the Database of Individual Seismogenic Sources, which was built, updated and maintained by the INGV DISS Working Group (DISS Working Group 2015). The most recent seismic zonation for the Italian territory (called ZS9, Meletti et al. 2008) relied in part on DISS and eventually led to the national SH map of Italy (MPS Working Group 2004). The database contains three
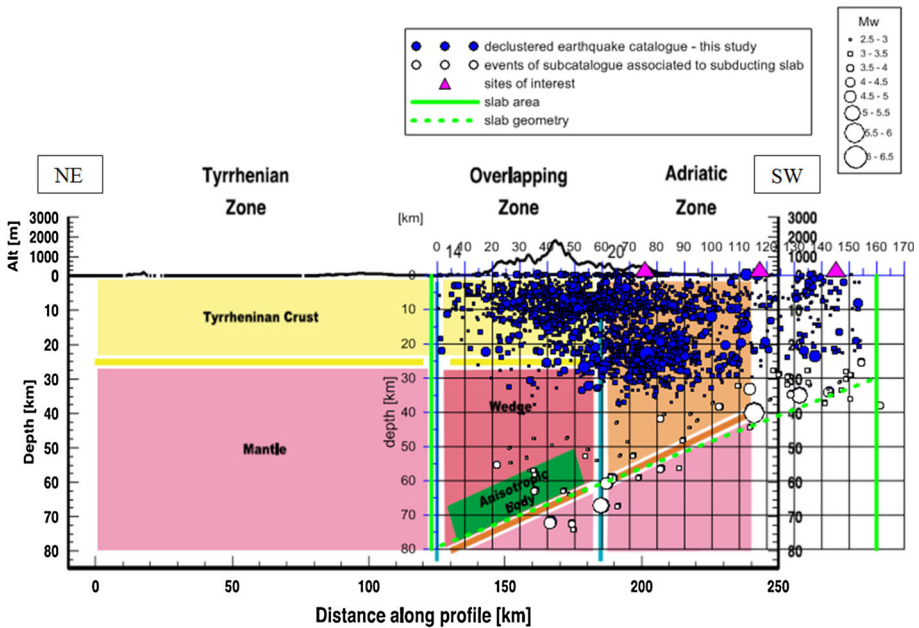
Fig. 3 2D schematic representation of the shallow and deep structures along a cross section of the Po Plain [modified after Bianchi et al. (2010)]

main types of seismogenic sources, namely: (1) individual seismogenic sources and (2) composite seismogenic sources.

Figure 4 shows the seismogenic sources of the Po Plain contained in DISS, as well as the location of the three sites considered in this study. The parameters of the seismogenic sources were derived from geological considerations, subsurface data analysis and from the historical and instrumental earthquake catalogues, that allow to constrain the expected magnitude (mainly through the observed/inferred length) and behavior of a given structure. The earthquake magnitude for each source is given in the moment magnitude scale (M_W), and represents the size of the largest earthquake that a seismogenic source can generate. The maximum magnitude is constrained by the largest historical earthquake that can be associated with that source, or the largest fault segment belonging to the source.

The data characterizing the composite seismogenic sources (CSS) include also the slip rate range calculated from geological and geodynamic considerations and, where possible, on the basis of the historical and instrumental seismicity.

2.4 Update of seismogenic source parameters, based on full 3D definition of active faults

The original geological work carried out within SIGMA consisted of the analysis of available subsurface data for the Po Plain aimed at the identification of buried active tectonic faults and folds, at their geometrical description and at the evaluation of their slip rate, with particular attention to areas surrounding the chosen reference sites (shown in Fig. 4).
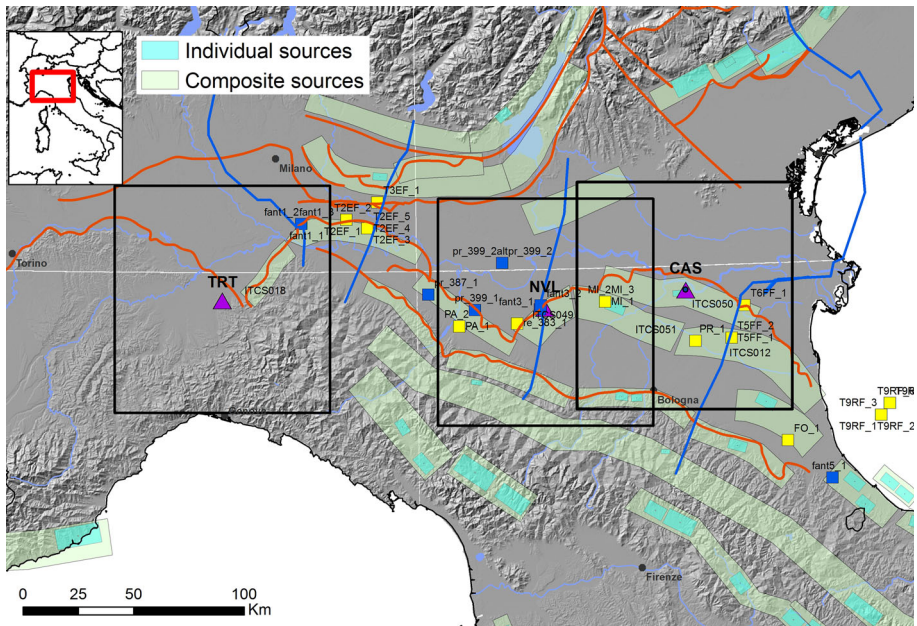
Fig. 4 Composite and Individual seismogenic sources of the Po Plain (from DISS). Note their position with respect to the reference sites of the project shown by *purple triangles*. Locations where fault slip-rate data have been analyzed (see Table 1) are shown as well by *yellow* and *blue* symbols. *Orange lines* show main thrust/reverse fault systems

The methodological approach used in the analysis consisted of a sequence of seven different main steps, i.e.: (1) study of the subsurface stratigraphic profile of the Po Plain; (2) construction of a GIS database including the available dataset; (3) conversion of the raster seismic lines to digital SEG-Y format; (4) analysis of the SEG-Y files for the identification of the key horizons and active faults; (5) time to depth conversion; (6) restoration of the deformation observed in the key horizons; (7) geometrical definition of active faults.

For the investigated structures it was possible to assess the slip rate value in a portion of the fault using 3D modeling of the available data. In particular, the slip rate values were obtained from the restoration of the deformation (both due to differential sediment compaction and to faulting and/or folding of the horizons) observed on the geological horizon on the hanging wall and footwall of the structures. The results of the analysis are summarized in Table 1. The individual locations where the geological slip rate analyses were performed, identified by Site ID in Table 1, are shown in Fig. 4.

The most relevant discrepancies between results from the new analyses and the DISS data concern the slip rate of the ITCS051 source (Novi-Poggio Renatico), which ranges between 0.83 and 1.15 mm/year in the new assessment, while in DISS is 0.25–0.50 mm/year. This source affects the SH of both Novellara and Casaglia (CAS) sites. Other significant sources for these two sites are ITCS049 (Reggio Emilia-Rolo), ITCS050 (Poggio Rusco-Migliarino) and ITCS012 (Malalbergo-Ravenna). The new geological assessments performed for these three sources substantially confirm the geometry and seismological parameters indicated in DISS, giving more detailed estimates of slip rates.

Table 1 Geometrical and seismological parameters of Po Plain seismogenic sources obtained by new analyses, in comparison with parameters available from the DISS database

This report

Site ID	Coordinates (decimal degrees) Lat	Lon	Dip (°)	Observed depth upper tip (km)	Age of horizons (Myr) min	max	Slip Rate (mm/yr)	Uncertainty (mm/yr)
fant1_1	45.199	9.338	40	1.0	0.0	1.8	0.08	0.03
fant1_2	45.199	9.338	40	1.0	1.8	2.6	0.33	0.08
fant1_3	45.199	9.338	40	1.0	2.6	3.6	0.36	0.06
T2EF_1	45.215	9.598	21-30	0.4-2.0	0	1.8	0.12	0.03
T2EF_2	45.215	9.598	21-30	0.4-2.0	1.8	5.3	1.07	0.02
T2EF_3	45.179	9.718	21-30	0.4-2.0	0	1.8	0.51	0.03
T2EF_4	45.179	9.718	21-30	0.4-2.0	1.8	2.6	0.56	0.08
T2EF_5	45.179	9.718	21-30	0.4-2.0	2.6	3.6	0.25	0.06
T3EF_1	45.285	9.777	25-45	1.05-1.7	0	1.8	0.19	0.03
pr_399_1	44.841	10.331	55	3.5	0.0	0.8	0.27	0.06
pr_387_1	44.907	10.065	36	1.9	0.0	0.8	0.23	0.06
PA_1	44.776	10.239	40	1.0	0	0.4	0.30	0.19
PA_2	44.776	10.239	40	1.0	0.4	0.8	0.42	0.19
pr_399_2	45.031	10.491	40	4.2	0.0	0.8	0.11	0.06
pr_399_2alt	45.031	10.491	15	5.2	0.0	0.8	0.32	0.06
re_383_1	44.783	10.571	40	2.0	0.0	0.8	0.10	0.06
fant3_1	44.839	10.702	56	1.78	0.0	1.8	0.20	0.03
fant3_2	44.855	10.707	12	4.67	0.0	1.8	0.96	0.03
MI_1	44.864	11.077	30	4.0	0	0.125	0.94	0.60
MI_2	44.864	11.077	30	4.0	0.125	0.4	0.83	0.27
MI_3	44.864	11.077	30	4.0	0.4	0.65	1.15	0.30
PR_1	44.695	11.587	40-45	1.0	0	0.65	0.36	0.12
T5FF_1	44.703	11.794	40	1.0	0	1.8	0.52	0.03
T5FF_2	44.703	11.794	40	1.0	1.8	3.6	0.41	0.03
T6FF_1	44.833	11.875	20-41	1.0-1.5	0	1.8	0.42	0.03
FO_1	44.278	12.094	40	3.0	0	0.65	0.31	0.12
fant5_1	44.118	12.338	30-60	0.94-2.25	0.0	1.8	1.04	0.03
T9RF_1	44.366	12.628	45-50	1.8	0	1.8	0.25	0.03
T9RF_2	44.366	12.628	45-50	1.8	1.8	2.6	0.63	0.08
T9RF_3	44.366	12.628	45-50	1.8	2.6	3.6	2.23	0.06
T9RF_4	44.412	12.680	45-50	1.8	0	1.8	0.11	0.03
T9RF_5	44.412	12.680	45-50	1.8	1.8	2.6	0.98	0.08
T9RF_6	44.412	12.680	45-50	1.8	2.6	3.6	0.43	0.06

DISS

DISS Source Code	Strike (°)	Dip (°)	Depth (km)	Rake (°)	Slip Rate (mm/yr)	Max mag
ITCS044	30-115	20-40	2-7	80-100	0.10-0.50	5.5
Not associated with any source						
ITCS009	120-140	20-40	2-8	90-120	0.10-0.50	5.6
Not associated with any source						
ITCS049	35-65	30-50	3-10	60-90	0.10-0.50	5.5
ITCS051	95-125	25-45	3-10	80-100	0.25-0.50	5.9
ITCS012	85-1150	20-40	2-8	80-120	0.10-0.50	5.6
ITCS050	85-115	25-55	1-8	80-100	0.10-0.50	5.5
ITCS011	95-145	20-40	3-8	80-100	0.10-0.50	5.9
ITCS039	120-140	25-35	3-7	80-100	0.10-0.50	5.7
Not associated with any source						

Site ID can be identified in Fig. 4

2.5 Uncertainty related to the historical earthquake catalogue

An important source of uncertainty in PSHA is related to the parameterization of historical macroseismic intensities. In several instances, the historical seismologist is not able to unambiguously assign a single intensity value that matches the observations.

A new parameterization of the historical catalogue in probabilistic terms was proposed (Mucciarelli 2014), introducing an expert judgment that rates the degree of belief on the macroseismic information. The influence of the intensity assignment uncertainty on PSHA was investigated considering two cities in the Po Plain (Ferrara and Modena), leading to the indication that the uncertainty in question propagates to PSHA affecting the result with a relative error of 25–30%.

3 Ground motion models

The selection of the ground motion prediction equations (GMPEs) appropriate to a specific regional geologic context is crucial for any SH evaluation, and one of the main tasks of the SIGMA WP2 was related to the selection and ranking of the most suitable GMPEs for the area of interest. The Po plain is a large sedimentary basin, with an area of about 50,000 km^2 and a sediment thickness varying from few tens of m to about 8 km; its geologic setting can affect the ground motion causing, among other things, amplification of the long period components and lengthening of the signals.

Every new earthquake reveals features of the seismic ground motion that were not taken into account in previous models because of scarcity of instrumental observations. For this reason the 2012 Emilia seismic sequence (with mainshocks M_W 6.1 on 20 May and M_W 6.0 on 29 May 2012) provided a vast amount of new strong motion data relevant to moderate magnitudes with 6 events of magnitude (M_W) larger than 5 (Luzi et al. 2013). The sequence was extensively recorded by strong-motion networks, operating in the Italian territory and neighbouring countries.

In the framework of the SIGMA project, an ad hoc strong-motion dataset for Northern Italy was compiled, also including records of the 2012 Emilia sequence that gradually were available (see Sect. 3.1). This dataset was then used both for the selection and ranking of existing GMPEs potentially applicable in the study (Sect. 3.2) and for deriving a regional GMPE (Sect. 3.3). Finally, sources of the ground-motion variability were investigated (Sect. 3.4). An updated review of all these aspects can be found in Lanzano et al. (2016), based on an enlarged strong-motion dataset, made available after the recent publications of Itaca v2.0 (ITACA Working Group 2016) and the Engineering strong motion database (Luzi et al. 2016).

3.1 Strong motion dataset

The latest version of the dataset assembled within SIGMA, called DBN2, consisted of 2174 waveforms exclusively from North Italy earthquakes, largely generated by thrust faults, encompassing from the destructive 1976 Friuli sequence to the 2012 Emilia sequence. This choice is considered consistent with the purposes of the present study, focused on the site-specific hazard assessment of selected sites in the Emilia region. It includes 136 earth-quakes (109 of them recorded by more than one station) and 299 stations (248 of them providing more than one record) in the $3.5 < M_w < 6.4$ range and epicentral distances

from 3.5 to 250 km. All the events are crustal, with depths of <30 km. The Emilia seismic sequence provided about 2/3 of the entire dataset. The selected records were processed uniformly applying the procedure proposed by Paolucci et al. (2011).

3.2 Selection and ranking of GMPEs

The previous strong motion dataset was used to select and rank a set of five candidate GMPEs. In order to identify the set of GMPEs to consider, indications obtained in the SHARE project (http://www.share-eu.org/, accessed July 12 2016) have been exploited considering the GMPEs selected for active shallow crustal region (ASCR) (Delavaud et al. 2012). Among the four models selected in SHARE for ASCR, the GMPEs developed by Cauzzi and Faccioli (2008) (CF08) and Akkar and Bommer (2010) (AB10) have been retained for the purpose of the present ranking.

In addition, the Boore and Atkinson (2008) model, including the modification proposed by Atkinson and Boore (2011) (BEA_M) was also considered. This GMPE is based on a global dataset and extended toward the lower magnitudes, therefore providing a tool better adapted for application in the region at study. We note in this respect that a minimum magnitude Mmin = 4.0 was used in PSHA in the first phase of the work, while this value was subsequently increased to 4.5 in the final calculations (see Sect. 4).

Lastly, two GMPEs specifically developed for Italy were included, i.e. Bindi et al. (2011) (ITA10), based on the Italian strong motion dataset recorded up to 2009, and Massa et al. (2008) (MS08), based on a dataset specific for Northern Italy, consisting of strong-motion data recorded up to 2007.

The log-likelihood (LLH) method by Scherbaum et al. (2009) was used to compare the recorded and predicted response spectra, which rates the applicability of a set of GMPEs to observed data by evaluating the differences between the logarithms of the observed and the predicted spectral ordinates. In this work, the GMPEs represent the models and the observations the data generating distribution: a small LLH will indicate that the candidate GMPE is close to the model that has generated the data, while a large LLH corresponds to a model that is less likely of having generated the data. The LLH (calculated for 23 periods in the range 0.04–4 s) was determined considering different subsets of DBN2 matching the range of validity of each GMPE. Figure 5 shows the LLH values as a function of period for the five GMPES that have been selected, considering a subset of the database (called DBNG). The ranking analysis indicates that the best overall performance is exhibited by the ITA10 and CF08 models.

Fig. 5 LLH values plotted as a function of period for the subsets of the DBNG database which include only records within the range of validity of each GMPE
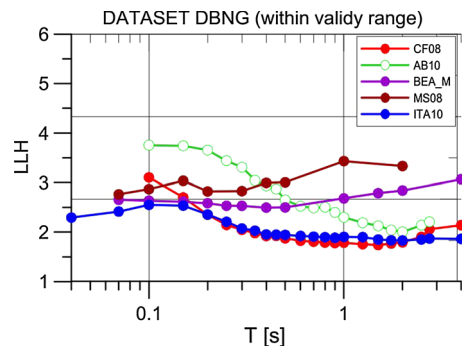
3.3 Establishing a GMPE for the Po Plain

A new GMPE suited for estimating the response spectral ordinates in the Po Plain was derived considering a parametric model with the functional form used by Bindi et al. (2011). The model parameters were derived for the geometrical mean of the horizontal components and the vertical component. The regressions were performed over the magnitude range 4–6.4 and considering both the Joyner and Boore and the hypocentral distances up to 200 km, and focal depths up to 30 km. This GMPE accounts for four different site classes, three of which are the A, B and C soil profile types from Eurocode 8 (EC8)—Part I. Furthermore, a new site class called C1 was introduced, which accounts for EC8 C-type sites that are located on the Po Plain deep sediments. Ground types D and E of EC8 were not considered as they are very poorly represented in the DBN2 database. The introduction of the C1 class is based on the observation that the waveforms observed at sites in the middle of the basin have uncommon features compared with the EC8-C class recordings, due to the relevant, and in many cases dominant, presence of surface waves.

The applicability of estimator parameters like Z1.0 or Z2.5 for deep basin effects developed for other datasets (like NGA-West 1, where the estimators in question were assessed mainly from oil exploration data from the Los Angeles basin) was not explored in detail because of the lack of the deep seismic velocity profiles required.

Four styles of faulting have been accounted for the earthquake sources, i.e. normal (NF), reverse (TF), strike-slip (SS) and unspecified (UN). The equations are derived for peak ground acceleration (PGA) and 5%-damped spectral accelerations (SA) over 24 periods in the period range between 0.04 and 4 s.

Figure 6 shows the comparison between the median predictions of the newly developed GMPE (black lines) and the pre-existing ITA10 (red lines) for PGA and spectral ordinates at periods 0.3, 1 and 4 s, and the observations (circular symbols) from recording sites on C1 ground type for thrust events of Mw 6.0. At long periods (T > 2 s) the GMPE developed for Po the plain predicts larger mean values than ITA10 up to 100 km, because of the low frequency amplification of the C1 soil class. The GMPE seems to fit adequately the observations, although the total standard deviation (sigma) is rather high, varying between 0.32 and 0.41 (log10 units), being largest at short periods.

The new GMPE improves the existing attenuation equations derived for Northern Italy. However it should be used considering that the DBN2 dataset is characterized by an unbalanced mix of recordings, i.e. a majority of thrust faulting data, class A and B sites at large distance and C1 sites at short distances. As a consequence, the GMPE derived in this study are appropriate for estimating the spectral ordinates in the Po plain area for C1 sites and thrust faulting. For other styles of faulting and soil categories the GMPEs derived by Bindi et al. (2011) is recommended and was actually used.

3.4 Analysis of ground motion variability

A residual analysis was performed in order to observe the different features of ground motion attenuation. The collected dataset highlights some peculiar features in the Po Plain region, such as: (1) low amplitudes at short periods; (2) attenuation with distance strongly dependent on frequency; (3) amplification of spectral ordinates in the distance range from 80 to 100 km, particularly evident at short periods (0.1 s); (4) strong low-frequency amplification at stations located on deep sediments (Luzi et al. 2013).
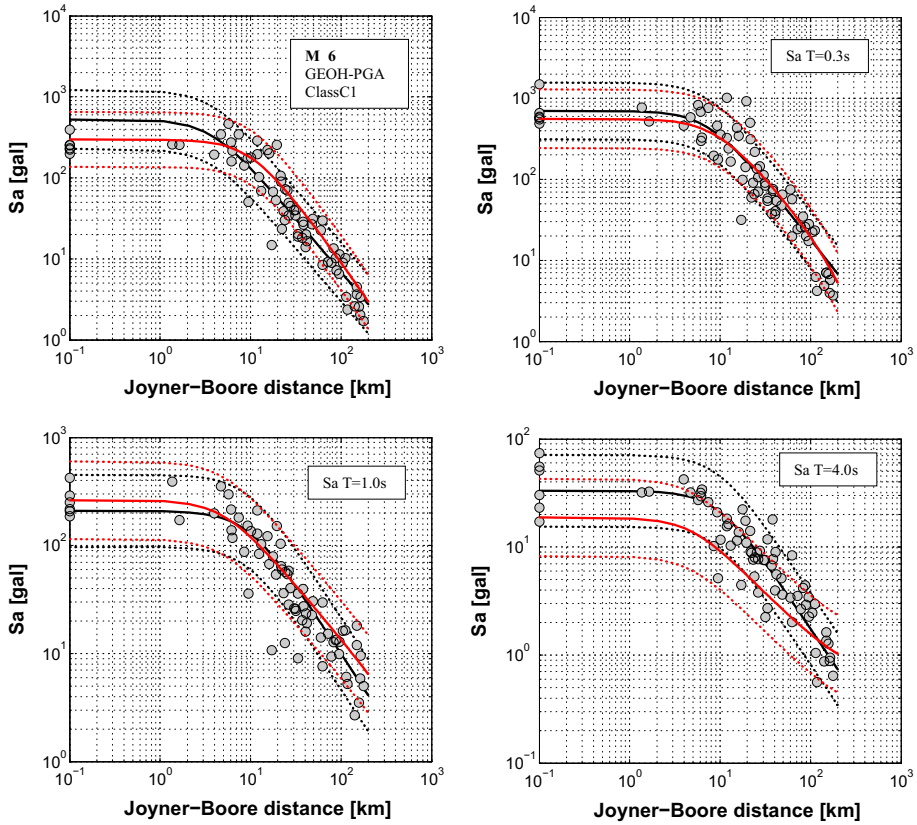
Fig. 6 Comparisons between median predictions and one standard deviation (*black curves*) for PGA and spectral acceleration at 0.3, 1.0 and 2.0 s and observations (*symbols*) for thrust focal mechanism. The *red curves* correspond to ITA10 predictions for C class. The observations are extracted from DBN2 in the magnitude range 6.0 ± 0.1

The sources of the ground-motion variability have been investigated with a view to implementing a partially "non-ergodic" approach in the PSHA. The method (and terminology) proposed by Rodriguez-Marek et al. (2011, 2014), afterwards applied by Luzi et al. (2014) to Italian strong-motion data, was followed. The total prediction residual (Δ_{es} where e stands for earthquake and s for site) has been separated into different variability contributions related to an event term (residual δB_e, with standard deviation τ), a site term (residual $\delta S2S_s$) and a site- and event-corrected term (residual δWS_{es}, with standard deviation $\phi_{ss,s}$, also referred to as "single-station phi"). The "total single station sigma" is given by:

$$\sigma_{ss,s} = \sqrt{\phi_{ss,s}^2 + \tau^2} \tag{1}$$

Herein, only a brief discussion is provided on the $\delta S2S_s$ and the $\phi_{ss,s}$ terms at the test sites selected for probabilistic hazard analysis. This discussion complements the more extended one given in Faccioli et al. (2015), focused on another typical Po Plain site (Mirandola), not originally included among the SIGMA tests sites.
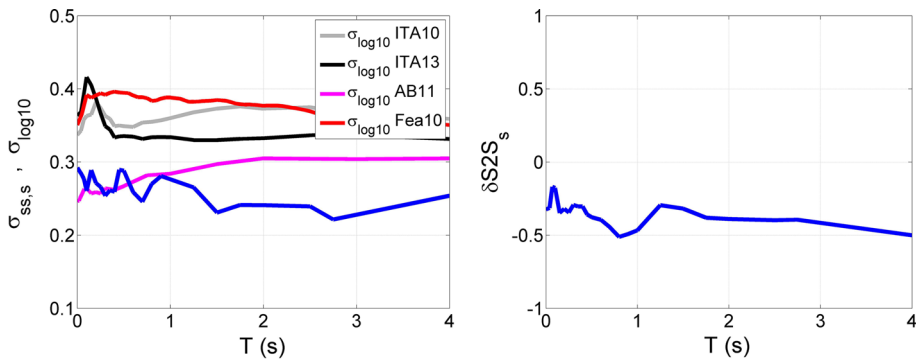
Fig. 7 (*Left*) Casaglia site: total single station sigma ($\sigma_{ss,s}$), *blue curve*, with total standard deviations of the GMPEs, all in base 10 logarithm, used in logic tree computations shown for comparison (i.e.: Bindi et al. 2011, and its 2013 modified version ITA13 developed for the Po Plain; Atkinson and Boore 2011, AB11; and Faccioli et al. 2010 modified version, Fea10). (*Right*) Ditto: site correction factor $\delta S2S_s$

Figure 7 shows the $\sigma_{ss,s}$ and $\delta S2S_s$ terms for the CAS site (identified/coinciding with the T0821 temporary station of INGV). The site term is a measure of the deviation of the average response at a site with respect to the average GMPE prediction for that site class, e.g. Eurocode 8 ground type C.

The station CAS exhibits a negative site correction factor, meaning that the site amplifies ground motions less than predicted by the GMPE for an average C-class site. Moreover, the total single site sigma is significantly smaller than the sigma of most of the GMPEs, and comparable (for T < 1 s) to the sigma of AB11. These differences, introduced through corrections to the GMPEs, will have a strong influence on the PSHA results. In particular, the reduction of sigma will combine with a substantially negative site correction factor, leading to a large decrease of the UH spectral ordinates.

4 Seismic hazard assessment

The SH assessment was performed in two phases: in Phase I, the influence of the epistemic uncertainties associated to some key input elements to the analysis (e.g. the model of extended seismic source zones, GMPEs, etc.) was explored. The results of Phase I PSHA constituted the baseline for evaluating the uncertainty reduction consequent to the improvements introduced in the second stage of the work. Phase II of the PSHA substantially extended the previous work (Phase I), by revising on one hand key input data and tools (influence of magnitude scale conversion, updating of earthquake catalogue, and of GMPEs), and, on the other hand, by providing a more ambitious treatment of uncertainties. This treatment was hinged on implementing the ground motion prediction task in PSHA through a partially non-ergodic ("single-site sigma") approach, verified through the adoption of a "generalized attenuation function" (GAF) approach, a simulation based method for predicting the ground motion hazard generated by complex fault systems.

4.1 Catalogue processing and activity rate computation

Since magnitudes of smaller earthquakes ($M < \sim 4.5$) are typically reported as local (M_L) or duration magnitudes, the reliability of the M_L–M_W magnitude conversion relationship

was investigated considering a selected set of magnitude data representative of the recent Po Plain seismicity, which are compared with existing correlations. The comparison showed that the M_L–M_W magnitude conversion relationship used in Phase I (taken from the CPTI11 earthquake catalogue, Rovida et al. 2011) is not suited for events with $M_W < 4.5$, because of clear overestimation of M_W. For this reason the regional working catalogue was updated (up to August 8, 2013) by keeping only $M_W \geq 4.5$ events. Thus, the use of a magnitude conversion relationship for the smaller magnitude events could be avoided because most of the $M_W \geq 4.5$ events prior to 2006 were directly taken from the CPTI11 catalogue, while M_W values of subsequent events ≥ 4.5 derive from a database of moment tensor solutions (http://cnt.rm.ingv.it/tdmt.html, Pondrelli et al. 2011). Consistently, since these findings apply for all seismogenic zones, updated Gutenberg-Richter parameters for generating new hazard results were derived using a minimum $M_W = 4.5$ (instead of 2.5, as in Phase I). The frequency–magnitude fits were improved with this choice, since starting from lower minimum magnitudes, as in Phase I, would have likely required a bilinear fit to appropriately adjust predictions to observations. The maximum magnitudes used in PSHA range from 6.5 (for most sources) up to 7.4 (for the two seismogenic sources of the Tuscany and Emilia Apennine, shown in subsequent Fig. 8).

By reducing the range of M_w values, the Gutenberg-Richter parameters, as well as their uncertainty, increase as expected. b-values were found to increase by about 11% for all Seismic Source Zones (SSZ), averaged, while activity rates (at M_w 4.5) increase by about 60%, leading to slightly more conservative results, i.e. about 10% in peak uniform hazard (UH) response at 10,000 years return period (RP).
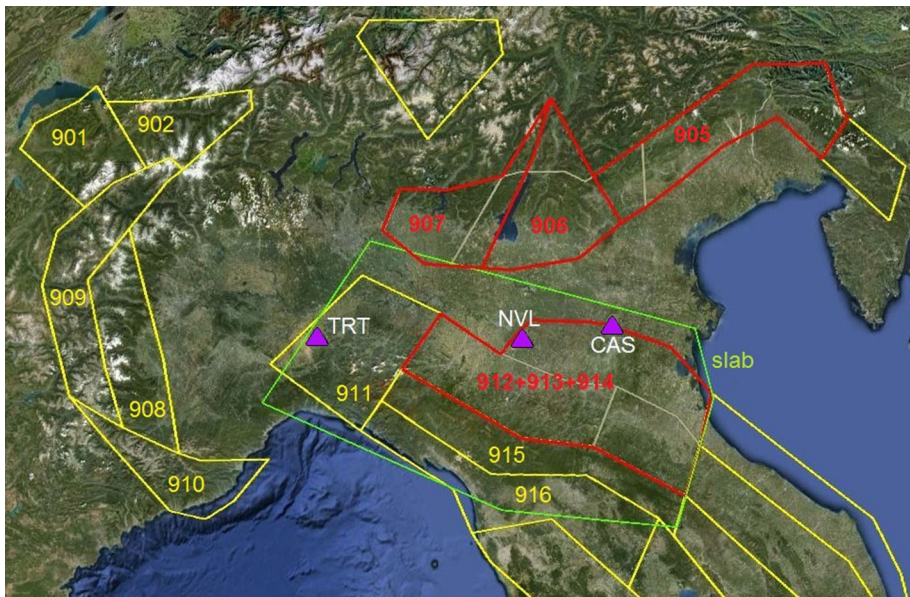

Fig. 8 Geometry of modified Seismic Source Zones (*red polygons*), compared with original ZS9 model (*yellow polygons*). *Purple triangles* show location of sites of interest. Shown in *green* is the deep (passive) subduction plane introduced in this study, labeled as *slab*. Numbered SSZs (together with slab) were used in the updated study

4.2 Single-station sigma approach

The GMPE describes the distribution of ground motion in terms of a median and a standard deviation of the logarithm of the prediction, often referred to as "sigma". The variability associated to GMPEs is among the largest in PSHA, and its impact on the probabilistic hazard level increases with the RP tending to become dominant at RPs of several 1000s of years, typically adopted for the earthquake resistant design of critical facilities. The "sigma" of the GMPE is computed under the "ergodic" assumption, whereby the ground motion uncertainty at a site is the same as the uncertainty computed from a large data set that includes ground motions from different sources and sites (Anderson and Brune 1999). The key to reducing the aleatory variability is to identify those components of ground motion variability at a single site that are repeatable rather than purely random, and to remove such components from the total sigma (Chen and Faccioli 2013).

For such reason, in parallel to the standard (i.e. ergodic) use of GMPE, a so–called partially "non-ergodic" (or "single-station sigma", see Rodriguez Marek et al. 2014) version was introduced in PSHA calculations. The single-station sigma approach requires modification of the GMPE predictions through site terms and the replacement the GMPE's sigma with the total single station sigma at a particular station. The site term ($\delta S2S_s$) is a random variable that represents the average within-event residual at station s. This term quantifies the average misfit of recordings from one particular site with respect to the event-corrected median ground-motion.

As discussed in Chen and Faccioli (2013), the $\delta S2S_s$ factor may in first approximation be considered as an intrinsic characteristic of the site and, as such, should be only moderately dependent from the GMPE used to calculate them, assuming that they employ the correct magnitude scaling. Likewise, the $\sigma_{ss,s}$ values seem not to be strongly affected by the choice of the specific GMPE introduced for the correction (Chen and Faccioli 2013), provided the scaling with respect to magnitude is about the same.

By using experimentally determined values of $\delta S2S_s$ and $\sigma_{ss,s}$ at specific sites, derived from a sufficient number of earthquake recordings, it is possible to implement the (partially) "non-ergodic" SH computation. This is performed by replacing the standard deviation of the GMPE (i.e. the "sigma") with the single-station standard deviation ($\sigma_{ss,s}$) value, whereas the site terms come into play as modifiers of the median predictions derived from the GMPEs:

$$\mu_{corrected}(T) = \mu_{GMPE}(T) \cdot 10^{\delta S2Ss(T)} \tag{2}$$

4.3 Seismic source models: area sources, fault sources and generalized attenuation functions

Different types of sources were considered for the PSHA, i.e. areal source zones (AS), smoothed/zoneless seismicity and fault sources (FS). The standard ZS9 AS model for Italy (Meletti et al. 2008) was modified by introducing:

1. significant changes to the geometry of the zones that include the central and the eastern Southern Alps (SSZs 905–907 of ZS9), as shown in Fig. 8;
2. merging of the zones including the Ferrara arc and the Pedeapenninic Thrust Front (SSZs 912–914);
3. a further dipping zone, below the SSZs from 911 to 916 of ZS9, to account for the Apennine deep seismicity.

Furthermore, a representation different from the ASs was used through an updated version of the smoothed seismicity model HAZGRID (Akinci 2010). This is a time-independent model based on gridded historical plus instrumental seismicity, that is spatially-smoothed to different length scales.

The third kind of source model are faults coupled with background (BG) seismicity. The latter is accounted for through area sources (ASs) with maximum magnitude bounded at 5.4 (residual magnitude not covered by the fault description). The FS include the CSS borrowed from the DISS (version 3.1.1) database, with modifications introduced following the WP1 results (see Sect. 2). A CSS is essentially an inferred structure based on regional surface and subsurface geological data, that are used to identify and map a complete fault system. It may either represent an identified fault limit or a significant structural change, implying that any CSS may span an UN number of potential individual ruptures, and be in principle able to generate earthquakes of any size, up to an assigned maximum magnitude. All CSS are characterized by geometric (strike, dip, depth) and kinematic (rake, slip rate, maximum magnitude) parametric descriptors.

CSS sources were first treated through the SH computational tool CRISIS2008 (Ordaz et al. 2013) as ASs with a simplified characteristic earthquake model with a truncated normal distribution for the characteristic earthquake magnitude, and Poisson occurrence. The main parameters used to model composite sources are the characteristic magnitude (Mc) and the mean recurrence time (RT). The latter designates the estimated recurrence intervals (or inter-event time) between similar-sized, maximum expected earthquakes on the composite source.

The "ideal" situation for a given fault segment would obviously be to carry a long list of associated earthquakes with clear neo-tectonic markers, so that statistics could be derived directly from observations. The actual observations of multiple, characteristic events on the same fault segment in Italy are definitely few, mostly represented by recent active sources in Central Apennines. Therefore, the RT has to be estimated by a combination of fault parameters. A widespread practice invokes the criterion of the "segment seismic moment conservation" (Field et al. 1999), by which:

$$RT = \frac{1}{Char\_Rate} = \frac{10^{(1.5Mc+9.05)}}{\mu V L W} \tag{3}$$

where RT is in years, Char_Rate is the annual mean rate of occurrence, μ is the shear modulus of the crustal rocks in N/m^2, V is the long-term slip rate on the fault in m/year, and L and W are the geometrical parameters of the fault, in km. The numerator of RT is the seismic moment associated to the characteristic earthquake, and the denominator the annual moment rate. Table 2 summarizes the relevant parameter values used to model the composite sources shown in Fig. 4.

Furthermore, an alternative approach was introduced to model fault-generated hazard for comparison and independent checking of the adopted modeling of FS, with special regard for near source locations. As a matter of fact, databases of most GMPEs tend to be insufficiently constrained at short distances and data may only partially account for the rupture process, wave propagation and complex 3D features. These characteristics can play a critical role when the sites at interest are located at source-to-site distances comparable with the fault dimension The alternative approach introduced is a novel one, appropriate for PSHA, and was proposed by Villani (2010) and Villani et al. (2014). The method generates synthetic ground motions from numerical simulations for selected earthquake scenarios, and these are introduced as input in the SHA as "non-standard" or

Table 2 Composite fault sources (CSS) from DISS3 used in the PSHA analysis, with Mc characteristic magnitude and RT recurrence time

CSS	Mc	L (m)	W (m)	Depth (km)	slip rate (mm/year)	RT (years)	Annual probability
ITCS050	6	11,482	7079	4.5	0.42	939	0.001065
ITCS051	6	11,482	7079	6.5	0.99	398	0.00251
ITCS049	6	11,482	7079	6.5	0.53	744	0.001344
ITCS012	5.6	6730	4853	5	0.44	561	0.001784
ITCS018	5.5	5888	4416	5	0.3	731	0.001368

Source depth is average between the smallest and largest depth of the CSS. Mc uncertainty was taken as 0.3 for all sources
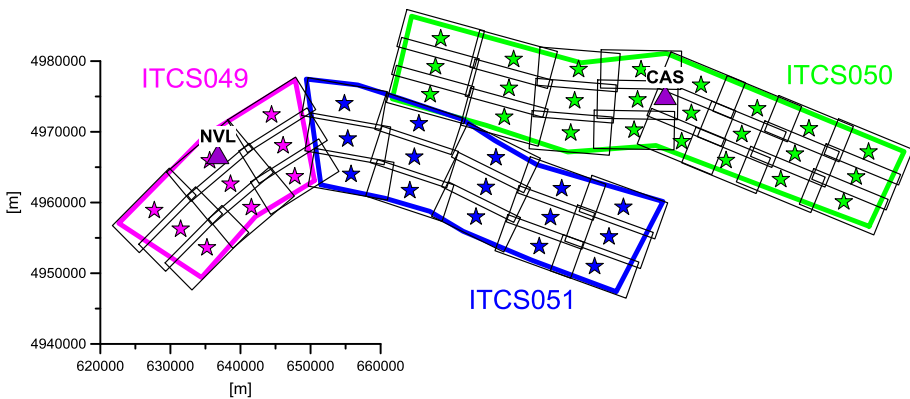
Fig. 9 Surface projection of the partition of CSSs ITCS049, ITCS050, ITCS051 into sub-sources, any of which was considered capable of generating a characteristic earthquake. *Triangles* show position of test sites

"generalized" description of attenuation (GAF). The GAF, actually replacing the empirically predicted values of GMPEs, were obtained from full time-domain simulations of fault rupture and propagation in a 1D Earth crustal structure, using the Exsim code (Motazedian and Atkinson 2005), specifically developed for stochastic finite-fault modeling of earthquake ground motions. Each CSS is partitioned into faults of equal size, consistent with the associated characteristic magnitude Mc, Fig. 9 shows the partition into subsources of the considered CSSs.

The method relies on a fairly large set of numerical source and wave propagation simulations at each site of interest, aimed at establishing realistic envelopes for near-source spectral acceleration levels. Results are then introduced in SHA in the form of median values and associated dispersion measures and then used to compute, as a function of position, the first two statistical moments of the intensity measure [response spectrum (RS) ordinate] considered in the analysis. These two moments become the main ingredients for the computation of the probability of exceeding a certain level of ground motion at a site, given the occurrence of a specific event (of magnitude m_i) on the considered k source (at distance r_k): $P(Y > y|m_i, r_k)$. When this term is computed through the use of numerical simulations, the predicted variability in the ground motion at a given site directly includes the 3D path and rupture features specific and unique to the studied site for a specified rupture (Graves et al. 2011). Hence, when the sigma is computed over a set of different

simulations of a specified earthquake scenario, at a particular site, such sigma really represents the (non-ergodic) variability of the ground motion amplitudes expected at a single site over many earthquake cycles on a given fault. Crucial for exploiting the foregoing approach is the ability of the PSHA tool used to handle occurrence probabilities according to the full probability theory formalism, instead of occurrence rates; this was implemented in the code CRISIS2008. The approach is thoroughly discussed in Villani et al. (2014), where interested readers can find more details.

4.4 Logic tree

Scientific (epistemic) uncertainties were considered by introducing through a logic tree alternative credible models or parameter values, and for each alternative model the hazard was separately computed, resulting in a suite of alternative hazard curves. The logic tree developed at this stage includes the source model (i.e. areas source, fault plus BG and diffuse seismicity) and the GMPEs. In phase II of the work, only GMPEs used in their non-ergodic mode were introduced, to better focus on the actual amplification features of the sites at study (as shown by the use of observations in the sophisticated, site specific, single station analyses), and to avoid possible double counting of uncertainties related to soil profile characteristics, when accounting for site specific effects in PSHA.

For the fault slip rates the mean values from Burrato et al. (2012) were adopted, i.e. uncertainties of epistemic nature in such values were not taken into account in the PSHA, to preserve a relatively light logic tree structure. Figure 10 shows the logic tree adopted for ground types C and A, with the weights assigned in phase II (for RPs of 2475 and 10,000 years).

The weights were assigned to the logic tree branches as ratings of the relative merits of the alternative models. As ITA13 and its earlier version ITA10 are scarcely constrained by data at the higher magnitude levels of our analyses ($M > 6.5$) we assigned a lower weight to the respective branches. For the weights assigned to the different earthquake source model branches, we used the results of the statistical performance of several hazard models for Italy tested versus strong motion observations (Albarello et al. 2015) with the highest scores gained by the gridded seismicity model used herein. For AS and FS + BG models,

Fig. 10 Logic tree adopted in Phase II, with weights assigned to each branch shown in *red*. Adopted GMPEs are: Faccioli et al. (2010) modified version (Fea10), Bindi et al. (2011) (ITA10), and its 2013 modified version (ITA13) and Atkinson and Boore (2011) (AB11)
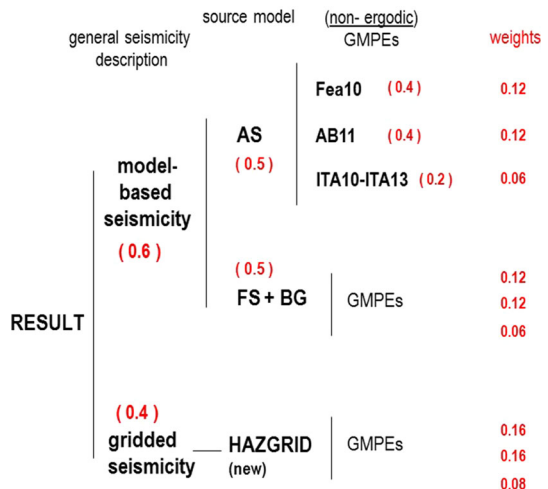
the results of separate analyses did not provide us any substantial reason to assign different weights.

4.5 Results

A borehole station was installed in CAS in the mid-90s by INGV (Margheriti et al. 2000) at the soil–bedrock interface at some 130 m depth, to exploit the detailed knowledge of the local underground geology available from oil exploration and the shallow depth of the top of the limestone and marl formations underlying the Quaternary sediments of the Plain at this particular location. This feature, occurring also at Mirandola (heavily hit the 2012 earthquakes), provided a rather unique opportunity to investigate bedrock motions in the Po Plain.

After the M5.4 Reggio Emilia earthquake of October 15 1996, a further instrument was added at the ground surface at CAS and after the Emilia mainshocks of May 20–29 2012, two new other temporary stations were installed at the same locations. More recently, a further instrument was installed in the vicinity of the OGS one, at few 100 m distance.

For all these reasons, CAS was selected as one of the benchmark sites for carrying out seismic site response analyses.

4.5.1 Comparing ergodic and non-ergodic approaches

Results obtained from a simple AS description of the earthquake sources, for Eurocode 8 ground category C, with GMPEs in both their "ergodic" and "non-ergodic" use (not shown here), disclose that the differences among amplitudes of the corresponding spectra strongly depend on those between the non-ergodic single-station sigma values ($\sigma_{ss,s}$) and the GMPE standard deviations. When the latter exceeds, for all periods, the site $\sigma_{ss,s}$ (as in the case of CAS, Fig. 7), the UH non-ergodic spectra are substantially decreased with respect to the ergodic ones.

Figure 11 compares, for the same AS description of the earthquake sources and for ground category A conditions, the influence of the "ergodic" versus "non-ergodic" treatment of the same GMPEs on the UH spectra. Note the drastic reduction in spectral amplitudes for all periods for the non-ergodic case. Such drastic reductions would not be normally expected: they occur at CAS because of the combined effect of two factors, both illustrated in Fig. 7. The first, stronger factor, is the reduction in the median prediction
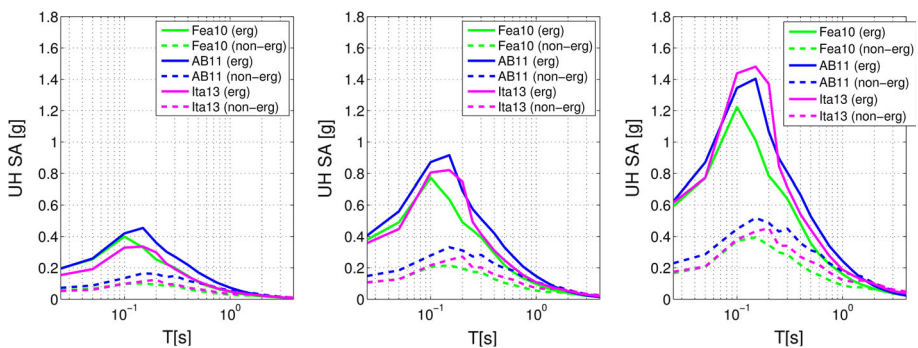

Fig. 11 CAS site, ground type A. UH acceleration spectra at return periods of 475, 2475 and 10,000 years, with ergodic and non-ergodic use of GMPEs (AB11, Fea10 and Ita13)

caused by the low site term ($\delta S2S_s$) values for exposed bedrock, estimated as the average of the site terms of the nearest accelerograph stations on rock, lying at >50 km distance in the Apennines (to the South of CAS). The second factor, as just stated, is a site-specific sigma ($\sigma_{ss,s}$) significantly lower than the standard deviation of most GMPEs. Note that considering as reference $\delta S2S_s$ on exposed bedrock, the average of the corresponding values on nearest rock stations, may be regarded as equivalent to retaining some degree of ergodicity.

4.5.2 Influence of area source versus fault source (plus background) representations

Figure 12 compares, in terms of UH spectra for ground type C, the results of fault + BG (FS + BG) and AS modeling, using the different GMPEs in their ergodic mode. The spectra are mostly quite comparable for 475 and 2475 years, while for 10,000 years RP the influence of the different GMPEs becomes more prominent. Actually, only the Fea10 GMPE generates an increase in hazard for the FS + BG modeling; this is because that GMPE enhances the contribution of the BG as magnitudes increase. With the AB11 GMPE the results are very similar for both approaches.

Next, the results of hazard analyses computed with the alternative GAF approach in terms of UH spectra, are compared with the case where the corresponding CSS are modeled as simple ASs with a characteristic earthquake behavior (as explained in Sect. 4.3). The CSSs involved in the computations are ITCS049, ITCS050 and ITCS051, with the model parameters shown in Table 2, using the three selected GMPEs (i.e. Ita13, Fea10 and AB11), in both their "ergodic" and "non-ergodic" use.

Comparisons of UH spectra from PSHA ergodic analyses with the GAF approach spectra are shown in Fig. 13 for RPs of 2475 and 10,000 years. Null spectra would be obtained for RPs of few 100s of years, because the resulting exceedance curves for the various spectrum ordinates saturate at the annual exceedance probability assigned to the characteristic earthquake of the CSS. In other words, the ground motion hazard tends to zero for RPs significantly smaller than the recurrence interval of the characteristic earthquake.

The results of the GAF approach are in reasonable agreement with AS results as far as peak spectrum level is concerned, when using GMPEs in their ergodic mode (see Fig. 13).
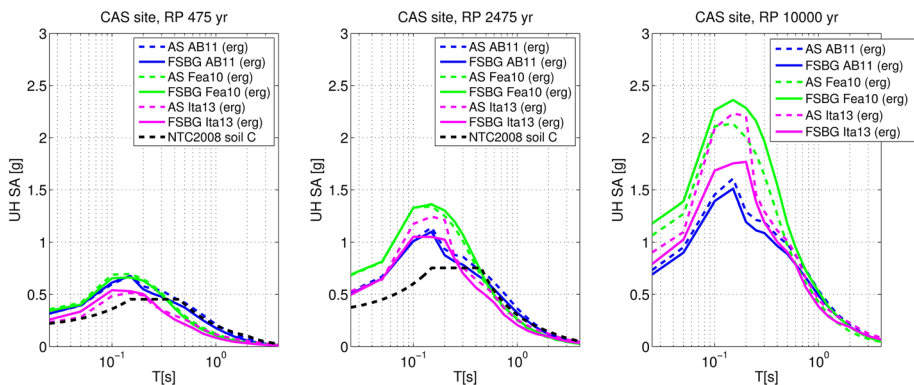

Fig. 12 CAS site, ground type C. Uniform hazard acceleration spectra (UH SA) at return periods (RP) of 475, 2475 and 10,000 years for different GMPEs are compared for the case of area source (AS) and fault source plus background (FSBG) source descriptions. Italian seismic code spectra (NTC 2008) shown as *thick dashed curves*
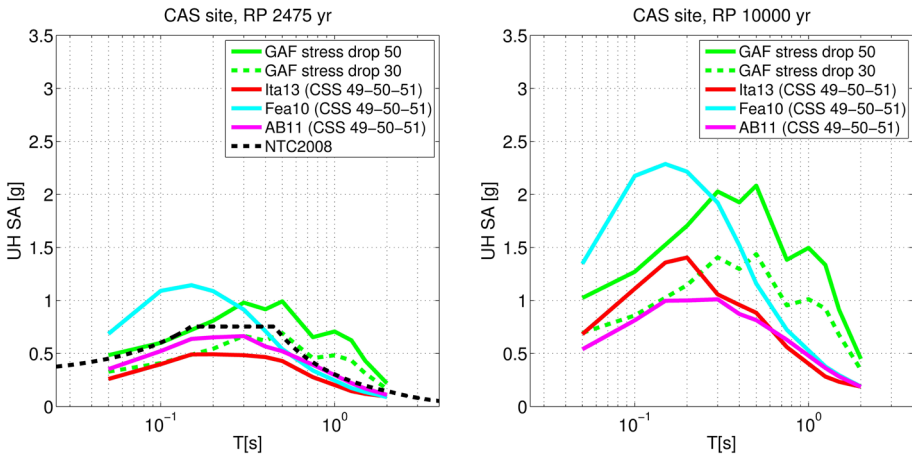
Fig. 13 CAS site. UH spectra from PSHA ergodic analyses with the fault sources modeled as area sources and characteristic earthquake model (labeled as *CSS*), compared with the GAF approach spectra for different stress drops

When GMPEs are used in their non-ergodic mode, as expected, GAF leads to significantly higher UH spectra (not shown), because it cannot reproduce the de-amplification associated to the site term $\delta S2S_s$ at CAS, shown in Fig. 7. For all cases, the intrinsic (and unavoidable) uncertainty in the stress drop seems to match the variability inherent in the use of traditional GMPEs. The use of the 1D site amplification function in the GAF enhances the amplification hazard at the typical resonance frequencies of the local site response, not necessarily seen by the GMPEs. As GAF spectra are strongly shaped by the site amplification function, this has to be carefully defined.

4.5.3 Results from logic tree and comparing UH spectra for Phase I and II analyses

The results of the logic tree calculations on ground type A are displayed in Fig. 14 as UH spectra, with the respective Italian seismic code (NTC 2008) spectra, where available.
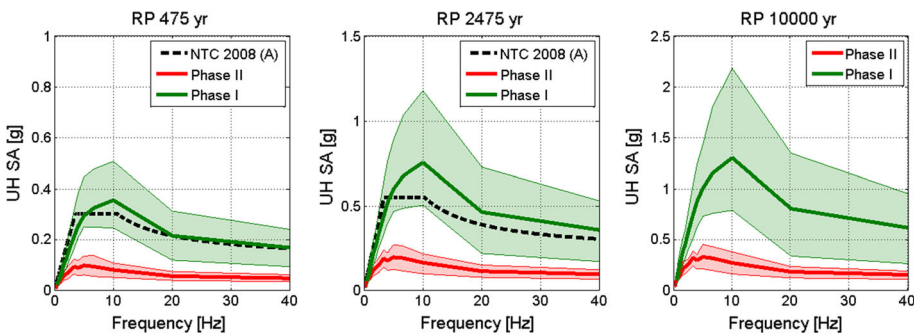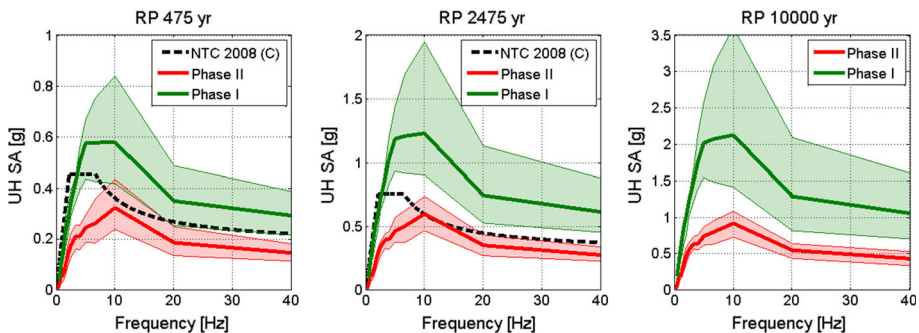

Fig. 14 CAS site: mean with 16- and 84-percentile uniform hazard (UH) acceleration spectra (SA) on ground type A at return periods of 475, 2475 and 10,000 years, from Phase II logic tree calculations (in *red*). Results from Phase 1 calculations (in *green*), and NTC 2008 code spectra (where available) are also shown for comparison

Phase I results are superimposed for comparison. The PSHA on ground type A indicates that:

- the exceedance curves (not shown) exhibit a roughly constant variability range with structural period; at 10,000 years RP the 84-percentile level spectrum peak at the CAS site reaches about 0.46 g, while the mean spectrum does not exceed 0.35 g (final results of Phase II);
- the comparison of the Phase II results with those of Phase I shows that the latter were much more conservative for all RPs, in terms of mean response spectra;
- the Italian (NTC 2008) code spectra for 475 and 2475 years RP always largely exceed the 84-percentile UHS of Phase II;
- while the variability increases with the RP, it is drastically reduced with respect to Phase I.

The results of the logic tree calculations on ground type C are displayed in Fig. 15 as UH spectra, with the respective NTC 2008 spectra, where available, and corresponding Phase I results.

The PSHAs on ground type C indicate that:

- all exceedance curves (not shown) exhibit a variability range increasing with structural period, from 0 s (where it is generally lower) to 3.0 s;
- at 10,000 years RP the peak of Phase II mean spectra reaches about 0.9 g at CAS site;
- the comparison of the present results with those of Phase I show different features depending on the site at study. At CAS, the non-ergodic use of GMPEs decreases significantly the spectral amplitudes;
- at CAS the variability of UH spectra is significantly reduced with respect to Phase I because of the transition from ergodic to non-ergodic sigma, but the results are significantly site dependent.

Generally speaking, the major factor explaining the reductions in variability and amplitudes, among Phase I and Phase II, is the transition from ergodic to non-ergodic sigma and, notably, the introduction of the site term $\delta S2S_s$.

Fig. 15 CAS site: mean with 16- and 84-percentile uniform hazard (UH) acceleration spectra (SA) on ground type C at return periods of 475, 2475 and 10,000 years, from Phase II logic tree calculations (in *red*). Results from Phase 1 calculations (in *green*), and NTC 2008 code spectra (where available) are also shown for comparison

5 Site effects

This section explores the approaches available to account for specific site effects in the framework of a probabilistic seismic hazard analysis (PSHA), with special emphasis on the application to the CAS site, selected for the reasons previously explained.

AS mentioned, the main geological feature affecting earthquake ground motion in the Po Plain is the presence of deep or very deep sediments, with depth of the top of Miocene formations rapidly increasing from about 100 m to some km (see Fig. 2). This context, coupled with a moderate seismicity, tends to produce:

- earthquake ground motion amplification at long periods;
- efficient generation of surface waves;
- moderate non-linear effects in seismic soil response, with possible liquefaction phenomena in the presence of loose saturated soils, as observed during the May 2012 seismic sequence.

5.1 Approaches to account for site effects (and related uncertainties) in PSHA

The seismic response features of a site may be quantified by site amplification functions (SAF), defined either by the Fourier or by the response spectral ratio of the response at the site divided by the corresponding response at the ideal outcropping bedrock (reference station), where available. Experimental evaluations of SAFs are in most cases limited by the lack of suitable reference stations in the vicinity of the site. This is an even more critical problem for the Po plain sites, where outcropping bedrock may lie tens of km away. For this reason, the experimental approaches for the evaluation of site-specific SAF have moved towards the use of single-station horizontal-to-vertical spectral ratios (HVSR). However, HVSRs cannot be easily used within a PSHA.

Following Cramer (2003), Bazzurro and Cornell (2004a, b), Perez et al. (2009), the approaches to account for seismic site effects within a PSHA can be broadly classified as shown in Table 3. Hybrid approaches typically combine the results of a PSHA at a rock site with a suitable site-specific SAF that multiplies the UH spectrum on rock. The SAF may be defined either by the amplification factors for generic sites introduced by national norms or guidelines (approach *HyG*), or by a site-specific evaluation, taken in most cases as the mean amplification function from 1D linear-equivalent wave propagation analyses for the soil profile at study (approach *HyS*). In the latter case, time-domain analyses are typically carried out with a suite of real input accelerograms, compatible with the target PSHA spectrum on rock. While *HyG* is the approach implicitly dictated by seismic norms,

Table 3 Classes of approaches to account for site effects in PSHA

Hybrid probabilistic/deterministic		Fully probabilistic	
Generic site (*HyG*)	Site-specific (*HyS*)	Generic site (*FpG*)	Site-specific (*FpS*)
PSHA on rock + SAF based on seismic norms	PSHA on rock + SAF based on site-specific soil response analyses (typically 1D)	PSHA based on GMPE with site correction factor	PSHA on rock + convolution with SAF conditioned to rock ground motion, typically based on 1D soil response analyses

HyS is frequently used for site-specific SH analyses of important facilities, so that we considered it as the reference approach for this study.

Although sound, and easy to grasp from an engineering point of view, the hybrid approach may provide exceedance rate estimates at the site not consistent with those on rock, as noted by Bazzurro and Cornell (2004b).

The previous limitation can be overcome by fully probabilistic approaches, intended for application either to a generic site (*FpG*) or to a specific site (*FpS*). *FpG* relies on the standard application of PSHA, where the site response is summarized within a period-dependent site factor that modifies the estimate of the considered (GMPE). Site factors are provided by practically all recent GMPEs [see e.g. the review in Douglas (2016)], associated to either broad soil categories, or to soil classes related to seismic norms, or to site-specific engineering parameters such as $V_{s,30}$. The drawback of *FpG* is that it may not provide reliable site-specific response evaluations. A site-specific GMPE could be used (e.g. Ordaz et al. 1994), if a sufficient strong-motion records are available at the site for a reliable GMPE to be derived, but this is seldom the case.

Finally, an *FpS* approach may be adopted, as proposed by Bazzurro and Cornell (2004b), involving the construction of conditional SAFs, i.e. of the site-specific ground motion amplification values at given vibration periods, conditioned to the exceedance of an assigned level of ground motion on rock.

In this work, attention was limited to the *HyS* approach, summarized through the following steps.

1. Start from a median uniform hazard response spectrum (UHRS) on rock for a given RP.
2. Select a set of real unscaled, or moderately scaled, accelerograms (e.g. seven of them are believed to suffice when moderate frequency scaling is operated) the average RS of which fits the median UHRS within, e.g. ±10% in a period range sufficiently large to encompass the peaks of the site-specific SAF.
3. Perform 1D wave propagation simulations, with nonlinear or linear equivalent soil models, using as input the accelerograms of step 2 and the best soil model based on an expert opinion.
4. Compute ratio of the RS of the output motions with respect to the rock motions; the resulting mean ratio will be taken as the mean amplification function of the site for the considered RP.
5. Obtain a design RS at ground surface by multiplying the rock UHRS by the site-specific SAF.
6. Quantify uncertainties, either under a logic tree framework discriminating the different model selections at steps 2 and 3, or by considering expert opinion.

A proper selection of input motions constrained to fit the target rock UHRS rock enables one to reduce significantly the scatter of results, so that the resulting SAF will be "conditioned" to the specific RP considered. This has the advantage of improving the control on the seismic response analyses, including non-linear effects, while keeping a reasonably low number of input motions.

5.2 Input motion selection

To guarantee proper selection of input ground motions for linear and non-linear seismic analyses of structures and soil systems (see ASCE/SEI 7-10 2010, for buildings and other structures, and ASCE/SEI 42-05 2007, for NPPs) the input accelerograms should:

- be records of real earthquakes approaching, in magnitude, distance and site-specific conditions, the combinations that mostly affect the site SH for the specific RP;
- exhibit an average RS approaching the target UHRS within, say, a −10 to +30% range [according to ASCE (42-05 2007)];
- be amenable to a moderate scaling, to improve the spectral matching with the UHRS, to be carried out in a period range sufficiently wide to constrain not only the spectral ordinate at the fundamental period of the structure, but the spectral shape as well (e.g. Baker and Cornell 2006).

The approach followed in this study (Smerzini et al. 2014) was based on a high-quality strong motion database (selected input motions for displacement-based assessment and design, SIMBAD), consisting of digital records of earthquakes relevant for SH studies in Italy, registered at stations with seismic site characterization, in most cases in terms of $V_{s,30}$. This was combined with a software for automatic selection of records compatible on average with a target spectrum, within a prescribed period range and tolerance. The software name is REXEL-DISP, available at www.reluis.it (accessed July 12, 2016).

Starting from the PSHA predictions on rock for CAS, seven unscaled accelerograms were extracted by REXEL-DISP from SIMBAD, to achieve an average broadband spectral compatibility from 0 to 8 s. Although the target spectrum is for ground category A, to increase the number of candidate records, these have been selected from both A or B ground types, with B sites characterized by relatively high $V_{s,30}$. Since strong motion records on type A sites are scantily represented in worldwide databases, it is reasonable that the soil class compatibility should be relaxed. Figure 16 shows an example of selection performed for the RP of 2475 years.

As a complementary step of the input selection, we also created a "spectrally matched" set of accelerograms. Starting from the previous selection, a scaling procedure in the frequency domain is applied, based on a correction factor calculated as the ratio of the RS of the accelerogram, with respect to the target one. Such correction factor is applied to scale iteratively the amplitude of the Fourier spectrum of the accelerogram, while keeping the same phase as the original one, until its RS fits the target one. The procedure is similar to that proposed by Shahbazian and Pezeshk (2010). Since the seed real accelerograms exhibit a broadband average spectral compatibility and are reliable also in the long period range, the scaling procedure does not usually introduce significant modifications in the
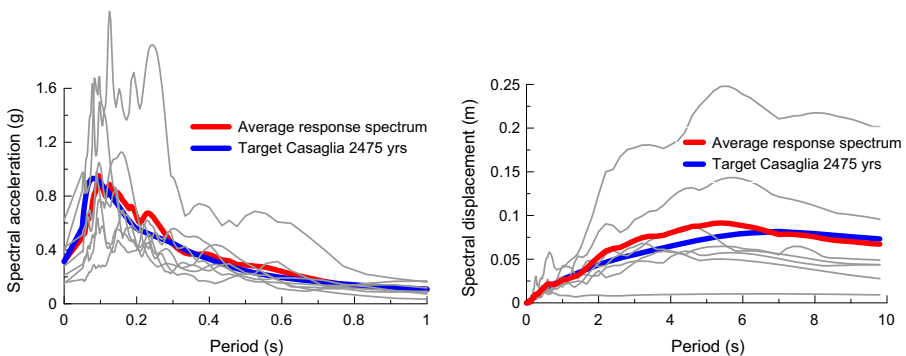

Fig. 16 Response spectra in acceleration (*left*) and displacement (*right*) of the accelerograms chosen for the Casaglia site for RP = 2475 years. *Horizontal* scales in the plots differ, to highlight the compatibility at short and long period

original record, either in terms of acceleration, or of velocity or displacement, as shown for one record in Fig. 17.

5.3 Site specific seismic response analysis and quantification of uncertainties

Given a target spectrum on rock, sources of uncertainties in site effects evaluation are mainly related to: (a) selection of input motions; (b) characterization of the soil profile dynamic properties; (c) selection of the method of analysis and computer code; (d) modeling and quantification of the non-linear soil behavior.

This section discusses and quantifies the epistemic uncertainty related to the:

- Vs soil profile;
- non-linear soil behavior and modelling approach;
- criteria for selection of input motion.

Concerning the Vs profiles, four models have been selected (see Table 4; Fig. 18), including seismic site characterizations carried out at the CAS site after the 2012 earthquakes. Since none of the experimental profiles could lead to reproducing in detail the peaks of observed spectral ratios (computed from weak motion data recorded at CAS at the surface and borehole location), an ad hoc Vs profile was adjusted and used.

For the non-linear soil modelling, four types of degradation curves were investigated (see Fig. 19), i.e. the Darendeli (2001) and the Ishibashi and Zhang (1993) curves, both accounting for dependence of the soil moduli on the mean confining pressure σ'_m; the mean standard curves of Seed and Idriss (upper limit) independent of σ'_m (Seed and Idriss 1970; Idriss 1990), and some available resonant column (RC) test results obtained from undisturbed samples at different depths extracted from borings in the general CAS area (DPC-INGV-S2 2013b, D8.1).

Concerning the input selection, different sets of real, scaled and unscaled accelerograms have been used in propagation analyses, as shown in Table 5.
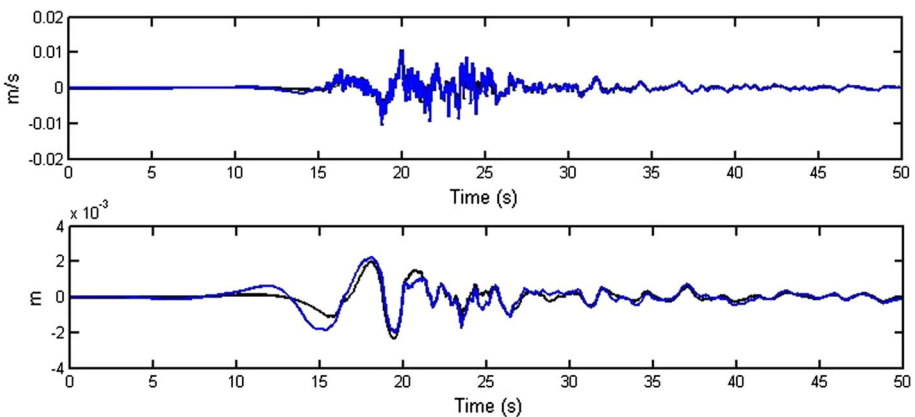

Fig. 17 Effects of spectral adjustment (in frequency content) of record i169x on the velocity (*top* graph) and displacement (*bottom* graph) waveforms. Shown in *black* is the original record, in *blue* the corrected one

Table 4 Summary of techniques of Vs survey at Casaglia, and site classification

Site	Type of measurement	V_{S30} (m/s)	Ground type
Fioravante and Giretti (2013)	Down hole + cross hole	201	C
Picozzi and Albarello (2007)	Inversion of Rayleigh wave dispersion and H/V spectral ratio curves	164	D
Margheriti et al. (2000)	Cross hole + inversions	191	C
DPC-INGV-S2 (2013a), D4.1	Cross hole	188	C
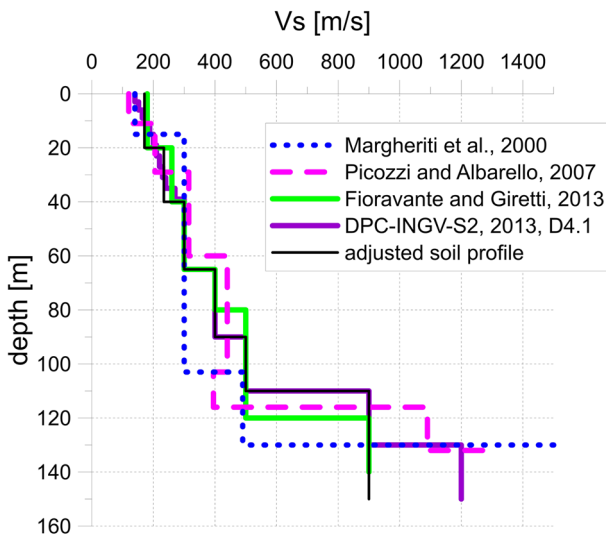
Fig. 18 Vs profiles measured in the Casaglia area, see Table 4. The Vs profile adjusted on the basis of the surface-to-borehole observed spectral ratios is also shown
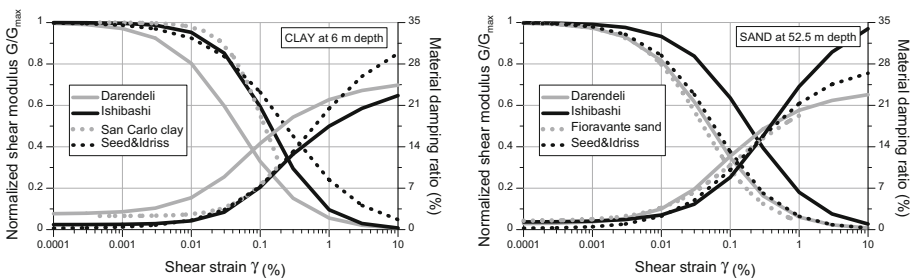
Fig. 19 Modulus reduction and damping curves for clay soils compared with RC test data (labeled *San Carlo* clay and *Fioravante* sand) obtained from samples at about 6 and 52 m depth

Table 5 Sets of accelerograms considered as input motions

1a	Real accelerograms with "broadband" spectral compatibility between 0.1 and 8 s
1b	Same as 1a, but scaled in frequency to closely match the target spectrum
2a	Real accelerograms with "narrow band" spectral compatibility between 0 and 1 s
2b	Same as 2a, but scaled in frequency to closely match the target spectrum

5.3.1 Effects of epistemic uncertainties in soil profile characterization and non-linear modeling

To quantify the effect of soil profile variability on the SAF, we carried out 1D linear equivalent numerical simulations, considering all the selected Vs profiles. To avoid superposition of input and Vs profile variability, we considered separately different input accelerograms from the set introduced in the previous sections. A representative set of results is shown in Fig. 20 for one of the input motions, but similar results were obtained also for the other input motions.

Relying on the adjusted Vs soil profile, and on the nonlinear soil degradation curves shown before, equivalent linear and non-linear analyses have been performed with the code DEEPSOIL 5.1 (Hashash et al. 2016). Representative results obtained with a specific input acceleration history as bedrock motion, selected and spectrally matched as previously explained, are shown in Fig. 21.

The surface spectra yielded by the NL analysis are generally more broadband than those from the LE analysis, exhibiting in particular higher short period ordinates. This difference depends to some extent on the input motion, but it should not be surprising in view of (a) the variety and complexity of stress–strain cycles generated by the NL motion, and (b) the fact that the LE description tends to generate pseudo-resonance at some specific frequencies (e.g. 0.13 and 0.21 s in the example of Fig. 21).

5.3.2 Effect of input motion selection on SAF variability

The Vs profile selected at CAS for this analysis was based on the Margheriti et al. (2000) investigations (rather than the one providing the best fit with borehole records), while the
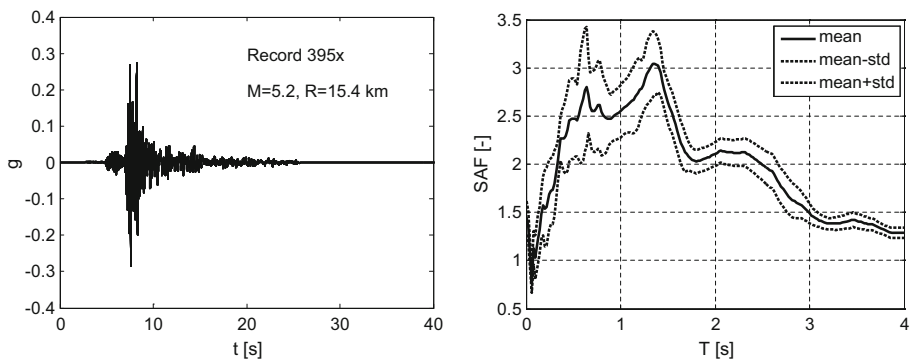

Fig. 20 *Left* input accelerogram, *right* SAFs computed on the response spectra by 1D linear equivalent analyses considering the different Vs profiles of Table 4
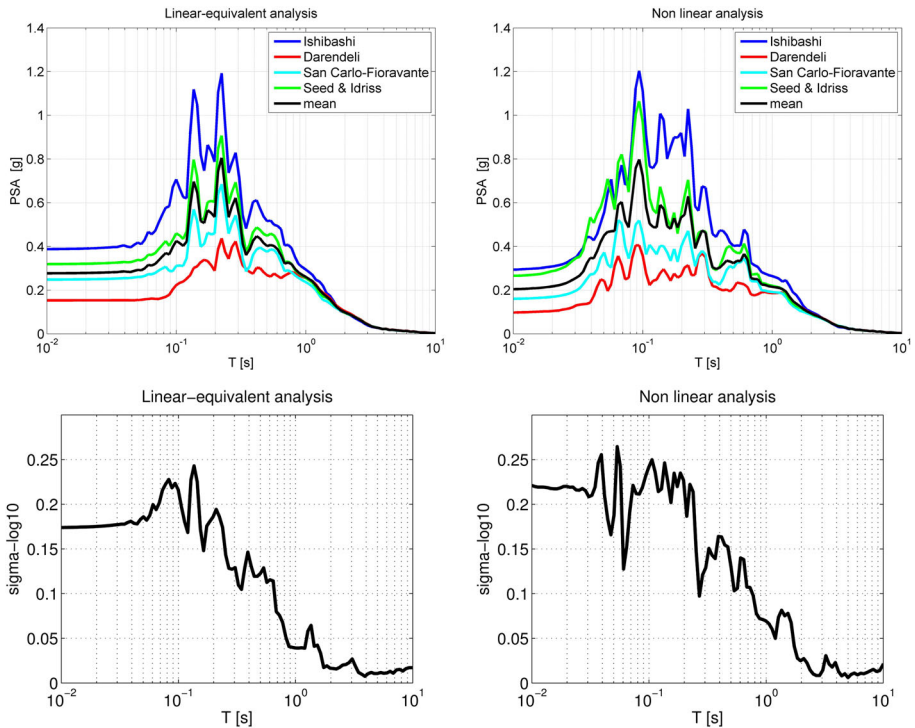
Fig. 21 *Top* response spectra at 5% damping obtained by 1D propagation analyses performed with selected acceleration input using the soil degradation curves summarized in Fig. 19. On the *left* side, results from linear equivalent analyses; on the *right* side: results from fully nonlinear analyses using DEEPSOIL numerical code. *Bottom* standard deviation ($\sigma_{\log10}$) of response spectra ordinates illustrated at *top*
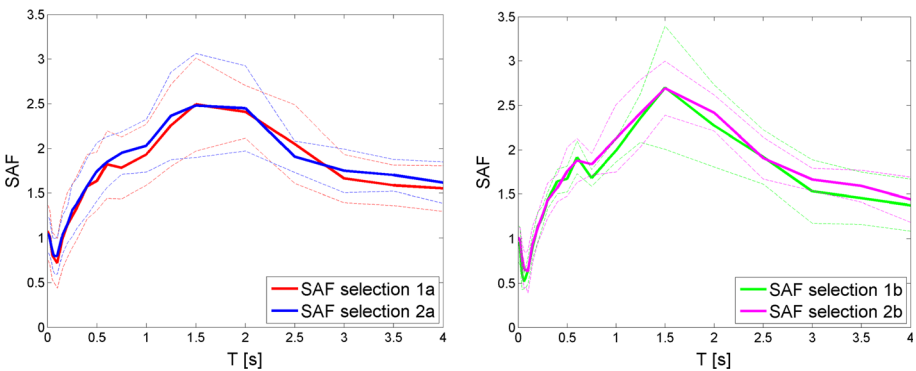

Fig. 22 Spectral amplification functions at CAS for the sets of records of Table 5. *Left* real records. *Right* adjusted (spectrally matched) records

linear equivalent approach was applied using the $G–\gamma$ and $\xi–\gamma$ curves fitting cyclic test data from soil samples of the Po plain (San Carlo + Fioravante, see Fig. 19).

Figure 22 shows the median spectral amplification functions calculated from the spectral ratio of the output versus input 5% damped response spectra. On the left side, the

comparison is shown for the real records dataset (1a vs. 2a in Table 5), while on the right side spectrally matched records were used (1b vs. 2b). No relevant differences are found for the two record sets in terms of mean SAFs, but the variability is significantly reduced in the short period range when using the corrected datasets.

As a conclusion we can state that:

- the epistemic uncertainty related to the mode of selection of input accelerograms is minor, in terms of real versus spectrally matched records, provided the response spectra of all sets are close to the target UHS on rock and the corrected records come from a "seed" set of real records approaching the rock UHS;
- the aleatory variability due to the different records in the same set is also minor, especially when spectrally matched records are considered (as expected).

5.4 Results

A summary of the assessments of the epistemic uncertainties inherent in the previous site response analyses is given in Table 6. The contribution of the NL modelling dominates the overall uncertainty, while the epistemic uncertainty related to the criterion for selection of input accelerograms was found to be negligible, provided that input motions, either real or spectrally matched, are compatible with the rock PSHA spectrum at the selected RP.

In interpreting these results, it should be understood that the quantification of σ_{NL} is only indicative, as it refers to the single soil profile considered and to the selected RP of 2500 years. A more comprehensive quantification of σ, related to the Mirandola site, can be found in Faccioli et al. (2015).

For the long period range, the related level of uncertainty is much smaller than in the short and intermediate period ranges. An obvious reason for such low values comes from the 1D modelling assumption itself, which considers vertical propagation of plane S-waves

Table 6 Contributions to the epistemic uncertainty in the UH response spectrum at CAS, $\sigma_{\log 10\ SA(T)}$, related to 1D soil modelling, with representative values given as a function of the period range

$\sigma_{\log 10\ SA(T)}$	Short periods (<0.5 s)	Intermediate periods (0.5–2 s)	Long periods (>2 s)
$\sigma_{Vs\ profile}$	0.07	0.05	0.03
σ_{NL}	0.19	0.08	0.02
σ_{input_1D}	Minor epistemic contribution to σ, provided input motions, either real or spectrally matched, are compatible with rock PSHA spectrum at the selected return period		
Total $\sigma_{epistemic\_1D} = (\sigma_{Vs}^2 + \sigma_{NL}^2)^{0.5}$	0.20	0.09	0.04
$\sigma_{PSHA\_rock}^a$	0.15	0.12	0.12
$\sigma_{tot} = (\sigma_{epistemic\_1D}^2 + \sigma_{PSHA\_rock}^2)^{0.5}$	0.25	0.15	0.13
$\sigma_{PSHA\_soil}^a$	0.09	0.13	0.13

σ_{PSHA_rock} and σ_{PSHA_soil} are the variabilities associated to the LT of Fig. 10, for ground type A and C respectively

[a] Computed as $[\log 10(UHS_{84th\ percentile}) - \log 10(UHS_{16th\ percentile})]/2$

in 1D horizontally layered media, disregarding complex site amplification effects related to source-to-site propagation path.

The total σ associated to a site-specific UHS, computed for example within a *HyS* approach (computed as explained in Sect. 5.1), would then be given by the following rule:

$$\sigma_{tot} = \sqrt{\sigma_{total\_epistemic}^2 + \sigma_{PSHA\_rock}^2} \tag{4}$$

where the epistemic contribution, derived from 1D (or more complex) analyses, is combined with the variability of the mean UH spectrum from the logic tree on rock for the selected RP.

Note that all the considered sources of uncertainty (input, soil profile, non-linear behavior) belong to the epistemic class, whereas the aleatory component is supposed to be already included in the PSHA results at rock.

As final results, Fig. 23 compares, for the CAS site, site specific PSHA results in terms of UH acceleration spectra, from the following approaches (see Table 3):

- PSHA on ground type A (labeled "rock LT");
- Fully probabilistic approach (*FpG*), from a purely non-ergodic tree (Fig. 10);
- 'Hybrid' site specific spectra (*HyS*), from combined (mean) results of PSHA on ground type A with 1D propagation analyses (linear-equivalent and non-linear), in red solid curves, with $\pm 1\sigma_{tot}$ band computed as shown in Table 6.

In Fig. 23, the mean UHS from the non-ergodic *Fp* and the *HyS* approaches are in reasonable agreement, although the *HyS* exhibits larger amplifications at long periods, as expected in the presence of the deep soil profile considered for the 1D simulations. However, the σ resulting from the *HyS* approach is much larger, owing to the combined epistemic uncertainties introduced in the modelling phase. We can conclude that the increased accuracy achieved by a site-specific approach, such as the *HyS*, is paid in terms of increased uncertainty of results, especially when the modelling assumptions involve large epistemic uncertainties, such as in the context of non-linear soil modelling.

Fig. 23 UHS at CAS for 2475 years return period. *Black dashed line* PSHA on ground type A. *Blue lines* site specific 2475-year, UH spectra resulting from non-ergodic use of GMPEs. *Red lines* average results from the *HyS* approach (considering both linear-equivalent and non-linear soil models). The $\pm 1\sigma$ bands associated to *HyS* results (σ_{tot}) are computed as shown in Table 6
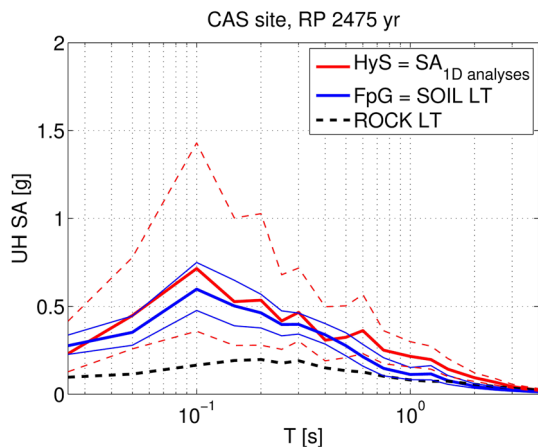
6 Concluding remarks

From among the extensive work carried out by the Italian group within the SIGMA project, discussed in its main aspects in the previous sections, the following main points deserve special attention by way of conclusive remarks and for future discussion:

(1) the comparative PSHA carried out with and without recurring to the single-station sigma approach at a representative, deep sedimentary site in the Po Plain;

(2) the so-called GAF approach for evaluating in a probabilistic context the ground motion hazard generated by rupture of faults belonging to CSS, and

(3) the in-depth assessment of the uncertainties tied to the site-specific hazard evaluation operated with a hybrid probabilistic/deterministic (HyS) approach.

The single-station sigma approach was applied in (1) to the site CAS disregarding the epistemic uncertainties associated to both the site-term ($\delta S2S_s$) and the single-station standard deviation ($\sigma_{ss,s}$). Their influence has been recently explored by Faccioli et al. (2015) on a site very similar to CAS as to subsoil characteristics and geological context, and the reader is referred therein for a detailed analysis. Peculiar to CAS is the fact that both its $\delta S2S_s$ and $\sigma_{ss,s}$ (Fig. 7) lie decidedly on the low side in a regional set of similar, deep sedimentary sites, all extensively recording the 2012 Emilia earthquake sequence. Such peculiarity explains the large differences between the ergodic and non-ergodic surface spectra (and their variability) at CAS. Even larger differences occur for exposed bedrock conditions, but in this case—in the absence of site records—$\delta S2S_s$ was taken as the average of the site terms at the nearest accelerometer sites on rock, lying at over 50 km distance from CAS. Such rock average $\delta S2S_s$ also turns out to be on the low side, but a very recent study (Lanzano et al. 2016), that includes earthquakes from different epicentral areas recorded between 2012 and 2015, has fully confirmed this tendency for CAS, thus dispelling doubts that single-station sigma parameters would be biased by single-path effects at rock stations. One key lesson from this analysis is that even at sites with very similar local geology and having the same seismotectonic context, such as those found at CAS and at the MRN site discussed in Faccioli et al. (2015), a non-ergodic hazard assessment can lead to large differences, likely caused by complex near-source and 3D propagation effects. In the absence of records, partial light on these differences can be shed through 3D numerical simulations.

Next, concerning (2), exploration of the GAF approach applied to the CAS site has indicated that the stress drop variability assumed in the fault rupture simulations, the shallow 1D crustal structure, and the regional geometric attenuation exerts a strong influence on the results, and that constraining these parameters with preliminary analyses against recorded data seems indispensable. The comparison with the ergodic standard PSHA results shows higher GAF response spectral levels at intermediate and long vibration periods, i.e. in the range where the GAF spectra also display peaks due to the dominant periods of the deep soil deposits. Interesting enough, the GAF results do not show the marked "de-amplification" features just discussed in relation to the site $\delta S2S_s$ and $\sigma_{ss,s}$ values.

Finally, as regards (3), an in-depth evaluation of the uncertainties associated to the site-specific analysis operated via a hybrid (HyS) probabilistic-deterministic approach has disclosed that the estimated surface spectra are affected by an estimation spread largely exceeding the spread from a non-ergodic PSHA, for periods <0.5 s, mostly as a result of the uncertainty linked to non-linear soil modeling. This would seem to support the choice

of obtaining through the *HyS* only the median surface spectrum, and associating to it the bedrock motion variability.

In important projects, reliance on cyclic test data from in situ soil samples seems to remain the most direct mean to reduce the soil modeling uncertainty (in 1D response analyses). However, in the absence of marked cyclic pore pressure effects, the severe "flattening" of surface spectra generated by current non-linear and equivalent linear calculations for medium and soft soil deposits for increasing excitation levels (up to, say, 0.3 g PGA) is not adequately supported by observational evidence.

Overall, the results of site-specific hazard evaluation indicate that, irrespective of the details by which the site effect is combined with the PSHA output on rock, the estimated site response can reach the peak amplitude levels resulting from PSHAs with GMPEs used in the non-ergodic mode. Nevertheless, the latter could lead to dominant site frequencies different from the 1D dominant frequencies of the hybrid approach (typically at lower frequencies). In the evaluation of the site response, the target bedrock spectrum for the selection of input THs to propagation analyses, and especially the shear modulus degradation and damping curves, turn out to be crucial and drastically affect spectral amplitudes of final results in the hybrid approach.

The results presented in this paper are believed to provide useful frameworks to be used in the future for PSHA analyses, as summarized in the overview document of the SIGMA project ("An Overview of the SIGMA Research Project—A European Approach to Seismic Hazard Analysis"), due for publication in mid-2017.

References

Akinci A (2010) HAZGRIDX: earthquake forecasting model for ML ≥5.0 earthquakes in Italy based on spatially smoothed seismicity. Ann Geophys 53(3):51–61. doi:10.4401/ag-4811

Akkar S, Bommer JJ (2010) Empirical equations for the prediction of PGA, PGV, and spectral accelerations in Europe, the Mediterranean Region, and the Middle East. Seismol Res Lett 81:195–206

Albarello D, Peruzza L, D'Amico V (2015) A scoring test on probabilistic seismic hazard estimates in Italy. Nat Hazards Earth Syst Sci 15:171–186

Anderson JG, Brune JN (1999) Probabilistic seismic hazard assessment without the ergodic assumption. Seismol Res Lett 70:19–28

ASCE/SEI 7-10 (2010) Minimum design loads for buildings and other structures. American Society of Civil Engineers, Reston. www.pubs.asce.org

ASCE/SEI 42-05 (2007) Evaluation of the seismic design criteria in ASCE/SEI Standard 43-05 for application to nuclear power plants. Brookhaven National Laboratory, Upton, NUREG/CR-6926

Atkinson G, Boore D (2011) Modifications to existing ground-motion prediction equations in light of new data. Bull Seismol Soc Am 101:1121–1135

Baker JZ, Cornell CA (2006) Spectral shape, epsilon and record selection. Earthq Eng Struct Dyn 35:1077–1095

Bazzurro P, Cornell CA (2004a) Ground-motion amplification in nonlinear soil sites with uncertain properties. Bull Seismol Soc Am 94(6):2090–2109

Bazzurro P, Cornell CA (2004b) Nonlinear soil-site effects in probabilistic seismic-hazard analysis. Bull Seismol Soc Am 94(6):2110–2123

Bianchi I, Park J, Piana Agostinetti N, Levin V (2010) Mapping seismic anisotropy using harmonic decomposition of receiver functions: an application to Northern Apennines, Italy. J Geophys Res 115:B12317

Bigi G, Bonardi G, Catalano R, Cosentino D, Lentini F, Parotto M, Sartori R, Scandone P, Turco E (eds) (1992) Structural model of Italy and gravity map 1:500,000. CNR Progetto Finalizzato Geodinamica. Sottoprogetto Modello Strutturale tridimensionale. Quaderni della Ricerca Scientifica 114, 3. Firenze, Italy

Bindi D, Pacor F, Luzi L, Puglia R, Massa M, Ameri G, Paolucci R (2011) Ground motion prediction equations derived from the Italian strong motion database. Bull Earthq Eng 9:1899–1920

Bommer JJ, Coppersmith KJ, Coppersmith RT, Hanson KL, Mangongolo A, Neveling J, Rathje EM, Rodriguez-Marek A, Scherbaum F, Shelembe R, Stafford PJ, Strasser FO (2015) A SSHAC level 3 probabilistic seismic hazard analysis for a new-build nuclear site in South Africa. Earthq Spectra 31(2):661–698

Boore D, Atkinson G (2008) Ground-motion prediction equations for the average horizontal component of PGA, PGV, and 5%-damped PSA at spectral periods between 0.01 s and 10.0 s. Earthq Spectra 24:99–138

Burrato P, Vannoli P, Fracassi U, Basili R, Valensise G (2012) Is blind faulting truly invisible? Tectonic-controlled drainage evolution in the epicentral area of the May 2012, Emilia–Romagna earthquake sequence (Northern Italy). Ann Geophys 55(4):525–531. doi:10.4401/ag-6182

Carminati E, Doglioni C (2012) Alps vs. Apennines: the paradigm of a tectonically asymmetric Earth. Earth Sci Rev 112:67–96

Cauzzi C, Faccioli E (2008) Broadband (0.05–20 s) prediction of displacement response spectra based on worldwide digital records. J Seismol 12:453–475

Chen L, Faccioli E (2013) Single-station standard deviation analysis of 2010–2012 strong-motion data from the Canterbury region, New Zealand. Bull Earthq Eng 11:1617–1632

Cramer CH (2003) Site seismic-hazard analysis that is completely probabilistic. Bull Seismol Soc Am 93(4):1841–1846

Darendeli MB (2001) Development of a new family of normalized modulus reduction and material damping curves. Ph.D. dissertation, University of Texas at Austin

Delavaud E, Cotton F, Akkar S, Scherbaum F, Danciu L, Beauval C, Drouet S, Douglas J, Basili R, Sandikkaya MA, Segou M, Faccioli E, Theodoulidis N (2012) Toward a ground-motion logic tree for probabilistic seismic hazard assessment in Europe. J Seismol 16:451–473

DPC-INGV-S2 (2013a) D4.1: site-specific hazard assessment in priority areas, Task 4 Working Group. https://sites.google.com/site/ingvdpc2012progettos2/home. Accessed 20 June 2016

DPC-INGV-S2 (2013b) D8.1: report on liquefaction phenomena and shaking causative levels, Task 8 Working Group. https://sites.google.com/site/ingvdpc2012progettos2/home. Accessed 20 June 2016

DISS Working Group (2015) Database of individual seismogenic sources (DISS), version 3.2.0: a compilation of potential sources for earthquakes larger than M 5.5 in Italy and surrounding areas. Istituto Nazionale di Geofisica e Vulcanologia.http://diss.rm.ingv.it/diss/

Douglas (2016) Ground motion prediction equations 1964–2016. Department of Civil and Environmental Engineering, University of Strathclyde, Glasgow, United Kingdom, 18th August, 2016. http://www.gmpe.org.uk/. Accessed 14 Feb 2017

Faccioli E, Bianchini A, Villani M (2010) New ground motion prediction equations for T > 1 s and their influence on seismic hazard assessment. In: Proceedings of the University of Tokyo symposium on long-period ground motion and urban disaster mitigation, Tokyo, Japan

Faccioli E, Paolucci R, Vanini M (2015) Evaluation of probabilistic site-specific seismic-hazard methods and associated uncertainties, with applications in the Po Plain, Northern Italy. Bull Seismol Soc Am 105(5):2787–2807

Fantoni R, Franciosi R (2010) Tectono-sedimentary setting of the Po Plain and Adriatic Foreland. Rend Fis Acc Lincei 21(1):S197–S209

Field EH, Jackson DD, Dolan JF (1999) A mutually consistent seismic-hazard source model for southern California. Bull Seismol Soc Am 89(3):559–578

Fioravante F, Giretti D (2013) Schede di caratterizzazione geotecnica dei principali litotipi. In: Martelli L, Romani M (eds) Microzonazione Sismica e analisi della condizione limite per l'emergenze delle aree epicentrali dei terremoti della Pianura Emiliana di Maggio-Giugno 2012 (ordinanza del commissario delegato-presidente della Regione Emilia_Romagna n. 70/2012), Relazione Illustrativa. Regione

Emilia-Romagna. http://ambiente.regione.emilia-romagna.it/geologia/temi/sismica/speciale-terremoto/sisma-2012-ordinanza-70-13-11-2012-cartografia#section-2. Accessed 14 Feb 2017

Graves R, Jordan T, Callaghan S, Deelman E, Field E, Juve G, Kesselman C, Maechling P, Mehta G, Milner K, Okaya D, Small P, Vahi K (2011) CyberShake: a Physics-based seismic hazard model for Southern California. Pure Appl Geophys 168(3–4):367–381

Hashash YMA, Musgrove MI, Harmon JA, Groholski DR, Phillips CA, Park D (2016) DEEPSOIL 6.1, User Manual. Urbana, IL, Board of Trustees of University of Illinois at Urbana-Champaign

Idriss IM (1990) Response of soft soil sites during earthquakes. In: Proceedings of the memorial symposium to honour Professor Harry Bolton Seed, Berkeley, California, vol II May **[as cited in the EERA Manual, Bardet et al. (2000)]**

Ishibashi I, Zhang XJ (1993) Unified dynamic shear moduli and damping ratios of sand and clay. Soils Found 33(1):182–191

ISIDe Working Group (2016) Version 1.0. doi:10.13127/ISIDe

ITACA Working Group (2016) ITalian ACcelerometric Archive, version 2.1. doi:10.13127/ITACA/2.1

Lanzano G, D'Amico M, Felicetta C, Puglia R, Luzi L, Pacor F, Bindi D (2016) Ground Motion prediction equations for region-specific PSHA. Bull Seismol Soc Am 106(1):73–92

Luzi L et al (2013) Overview on the strong-motion data recorded during the May–June 2012 Emilia seismic sequence. Seismol Res Lett 84:629–644

Luzi L, Puglia R, Russo E, ORFEUS WG5 (2016) Engineering Strong Motion Database, version 1.0. Istituto Nazionale di Geofisica e Vulcanologia, Observatories & Research Facilities for European Seismology. doi:10.13127/ESM

Luzi L, Bindi D, Puglia R, Pacor F, Oth A (2014) Single-station sigma for Italian strong-motion stations. Bull Seismol Soc Am 104(1):467–483

Margheriti L, Azzara RM, Cocco M, Delladio A, Nardi A (2000) Analysis of borehole broadband recordings: test site in the Po Basin, Northern Italy. Bull Seismol Soc Am 90(6):1454–1463

Massa M, Morasca P, Moratto L, Marzorati S, Costa G, Spallarossa D (2008) Empirical ground-motion prediction equations for Northern Italy using weak- and strong-motion amplitudes, frequency content, and duration parameters. Bull Seismol Soc Am 98:1319–1342

Meletti C, Galadini F, Valensise G, Stucchi M, Basili R, Barba S, Vannucci G, Boschi E (2008) A seismic source zone model for the seismic hazard assessment of the Italian territory. Tectonophysics 450:85–108

Motazedian D, Atkinson GM (2005) Stochastic finite-fault modeling based on a dynamic corner frequency. Bull Seismol Soc Am 95(3):995–1010

MPS Working Group (2004) Redazione della mappa di pericolosità sismica prevista dall'Ordinanza PCM del 20 marzo 2003. Rapporto Conclusivo per il Dipartimento della Protezione Civile, INGVMilano-Roma, 04/2004, 65 pp.+5 appendici

Mucciarelli M (2014) Uncertainty in PSHA related to the parametrization of historical intensity data. Nat Hazards Earth Syst Sci 14:2761–2765

NTC (2008) Norme tecniche per le costruzioni, 2008. DM 140108. *Ministero delle infrastrutture, Gazzetta Ufficiale,* 29, 4.2.2008, Rome

Ordaz M, Singh SK, Arciniega A (1994) Bayesian attenuation regressions: an application to Mexico City. Geophys J Int 117:335–344

Ordaz M, Martinelli F, D'Amico V, Meletti C (2013) Crisis 2008: a flexible tool to perform probabilistic seismic hazard assessment. Seismol Res Lett 84:495–504

Paolucci R, Pacor F, Puglia R, Ameri G, Cauzzi C, Massa M (2011) Record processing in ITACA, the new Italian strong-motion database. In: Akkar S, Gülkan P, van Eck T (eds) Earthquake data in engineering seismology. Geotechnical, geological, and earthquake engineering, vol 14. Springer, pp 99–113

Perez A, Jaimes MA, Ordaz M (2009) Spectral attenuation relations at soft sites based on existing attenuation relations for rock sites. J Earthq Eng 13:236–251

Picozzi M, Albarello D (2007) Combining genetic and linearized algorithms for a two-step joint inversion of Rayleigh wave dispersion and H/V spectral ratio curves. Geophys J Int 169(1):189

Pondrelli S, Salimbeni S, Morelli A, Ekström G, Postpischl L, Vannucci G, Boschi E (2011) European-Mediterranean regional centroid moment tensor catalog: solutions for 2005–2008. Phys Earth Planet Inter 185(3):74–81

Renault P (2014) Approach and challenges for the seismic hazard assessment of nuclear power plants: the Swiss experience. Boll Geofis Teor Appl 55(1):149–164

Rodriguez-Marek A, Montalva GA, Cotton F, Bonilla F (2011) Analysis of single-station standard deviation using the KiK-net data. Bulll Seismol Soc Am 101(3):1242–1258

Rodriguez-Marek A, Rathje E, Bommer J, Scherbaum F, Stafford P (2014) Application of single-station sigma and site response characterization in a probabilistic seismic-hazard analysis for a new nuclear site. Bull Seismol Soc Am 104(4):1601–1619

Rovida A, Camassi R, Gasperini P, Stucchi M (eds) (2011) CPTI11, the 2011 version of the parametric catalogue of Italian earthquakes. Istituto Nazionale di Geofisica e Vulcanologia, Milano

Scherbaum F, Delavaud E, Riggelsen C (2009) Model selection in seismic hazard analysis: an information-theoretic perspective. Bull Seismol Soc Am 99:3234–3247

Seed HB, Idriss IM (1970) Soil moduli and damping factors for dynamic response analysis, Report No. UCB/EERC-70/10. University of California, Berkeley **[as cited in the EERA Manual, Bardet et al. (2000)]**

Senfaute G (2012) Research and development programme on seismic ground motion assessment: SIGMA. In: International experts meeting on protection against extreme earthquakes and tsunamis in the light of the accident at the Fukushima Daiichi Nuclear Power Plant (IEM3). IAEA Headquarters Vienna, Austria 4–7 September 2012

Shahbazian A, Pezeshk S (2010) Improved velocity and displacement time histories in frequency domain spectral-matching procedures. Bull Seismol Soc Am 100:3213–3223

Smerzini C, Galasso C, Iervolino I, Paolucci R (2014) Ground motion record selection based on broadband spectral compatibility. Earthq Spectra 30(4):1427–1448

Swissnuclear (2013) Probabilistic seismic hazard analysis for Swiss nuclear power plant sites—Pegasos Refinement Project. Final report, vol I (summary report). http://www.swissnuclear.ch/upload/cms/user/PEGASOSProjectReportVolume1-new.pdf. Accessed 14 Feb 2017

Villani M, Faccioli E, Ordaz M, Stupazzini M (2014) High-resolution seismic hazard analysis in a complex geological configuration: the case of the Sulmona Basin in Central Italy. Earthq Spectra 30(4):1801–1824

🖄 Springer